

Charmonium in the instantaneous approximation

Johan Linde* and Håkan Snellman†

Department of Theoretical Physics

Royal Institute of Technology

S-100 44 STOCKHOLM

SWEDEN

Abstract

The charmonium system is studied in a Salpeter model with a vector plus scalar potential. We use a kinematical formalism based on the one developed by Suttrop [1], and present general eigenvalue equations and expressions for decay observables in an onium system for such a potential both in the Feynman and Coulomb gauges. Special attention is paid to the problem with renormalization of the lepton pair decays, and we argue that they must be defined relative to one of the experimental decay widths because renormalization of the vertex function is not possible. The parameters of the model are determined by a fit to the mass spectrum and the lepton pair decay rates. Two gamma decays and E1 and M1 transitions are then calculated and found to be well accounted for. No significant differences in the results in Feynman or Coulomb gauge are found. A comparison is made, regarding the electromagnetic transitions, between the full and reduced Salpeter equation. A large difference is found showing the importance of using the full Salpeter equation.

PACS: 11.10.St 13.40.Hq 13.20.Gd

Keywords: Salpeter equation, charmonium, electromagnetic decays, lepton pair decays, renormalization

Typeset using REVTeX

*E-mail: jl@theophys.kth.se

†E-mail: snell@theophys.kth.se

I. INTRODUCTION

The Bethe-Salpeter formalism has recently been used in various ways in more careful investigations of quarkonium physics. For example Munczek and Jain [2] have used the full Bethe-Salpeter equation together with the Schwinger-Dyson equation to study the mass spectrum and lepton pair decays of light and medium-heavy mesons, Resag *et al.* [3–6] have written a series of papers about the Salpeter equation where they have studied mass spectra and various decay observables for both light and heavy mesons, Kugo *et al.* [7] have calculated the Isgur-Wise function and Harada and Yoshida have calculated the QCD S parameter [8] and developed a method to solve the full Bethe-Salpeter equation [9]. The stability of the Salpeter equation for various Lorentz structures of the confining potential has been studied by Olsson *et al.* [10] and Parramore *et al.* [11,12]. Olsson *et al.* have also studied the validity of the reduced Salpeter equation [13].

In this paper we undertake an investigation of the radiative decays of the lowest charmonium levels including both M1 and E1 transitions in our study as well as the two-gamma decays of the corresponding pseudoscalar, scalar and tensor states.

Like many other authors [3,14,15] we use the instantaneous approximation of the Bethe-Salpeter equation – the Salpeter equation – which has a well defined physical interpretation. Our kinematical analysis uses a formalism based on the one developed by Suttorp [1]. (Another formalism in a similar spirit has been developed by Lagaë [16].) This leads to a set of coupled equations for the amplitudes which are solved numerically. In this paper we present a general set of eigenvalue equations and decay amplitudes for lepton pair decays, two gamma decays and E1 and M1 transitions, which can be used in any model with a vector plus scalar potential using the formalism of Suttorp.

Our potential consists of one short-range vector part describing the one-gluon-exchange interaction and one scalar long-range confining part. Investigations of the stability of the Salpeter equation for confining potentials with various Lorentz structures have shown that for light quarks there are no stable solutions for a scalar confinement [10–12]. This problem does not appear for heavy quarks like the charm quark. Furthermore a Lorentz time component vector confinement, which has been shown to be the most stable one, gives a contribution to the spin-orbit coupling with the wrong sign. We have therefore chosen a scalar confinement potential.

In quantum mechanics the spectrum itself does not uniquely determine the potential. We also need as input some other information concerning the localization of the system, such as the value of the wave function close to the origin. As input we therefore take the energy levels of the charmonium spectrum as well as the decay rates of the vector 1^{--} states into lepton pairs.

The instantaneous approximation leads, strictly speaking, to some problems with renormalization, since the Ward-Takahashi identities are then not relevant for the renormalization of the vertex function in the lepton pair decay. Furthermore the kernel is confining and contains a dimensionful coupling constant for the confining part. This leads in the final analysis to a renormalization procedure where we use the decay width for $J/\Psi \rightarrow e^+e^-$ to define the renormalization constant. Thus, we calculate the ratios of the decay rates of the vector states into lepton pairs, rather than the rates themselves.

We adopt the formalism of Mandelstam [17] to calculate the radiative decay amplitudes.

The gauge invariance of this method in the instantaneous approximation is not obvious, but in Sec. VI we show that the decay amplitudes are indeed gauge invariant.

The paper on heavy quarkonia by Resag and Münz [5] overlaps to some extent with our paper. They have also used a Salpeter model to calculate mass spectra and decay observables for charmonium. However, they have used a somewhat different potential. In particular, they have introduced a cut-off in the potential at the origin in order to renormalize the lepton pair decay widths. In this paper we discuss the difficulties of renormalization and conclude that an experimental decay width has to be used to properly define the renormalization. A cut-off also necessitates some extra parameters in the model, and they obviously affect the results. In particular, the lepton pair decay widths depend on the wave function's value at the origin, and therefore one can obtain any value for those by varying the cut-off parameters.

In addition, we present general equations in a formalism different from [5] and investigate the importance of non-dominant terms in the wave functions.

The outline of our paper is as follows. In Section II we briefly discuss the Bethe-Salpeter equation to define our variables. In Section III we describe the potential used in the model. We use a short-range Coulomb potential plus a long-range confining linear potential. In Section IV we give the expression for lepton pair decay and discuss the problem with renormalization. In Section V we give the expressions for the $\gamma\gamma$ decays and in Section VI we give the expressions for the M1 and E1 transitions. There we also discuss the gauge invariance in the instantaneous approximation. In Section VII we present the numerical results and finally in Section IX we give a summary of our results and conclusions.

II. THE SALPETER EQUATION

The wave function $\chi(q)$ for bound states of a fermion-antifermion pair satisfies the spinor Bethe-Salpeter equation

$$(\not{q} + \frac{P}{2} - m)\chi(q)(\not{q} - \frac{P}{2} - m) = i \sum_{i=1}^5 \int \frac{d^4 p}{(2\pi)^4} K^i(p, q, P) \Gamma^i \chi(p) \Gamma^i. \quad (1)$$

Here, P is the momentum of the bound state and q is the relative momentum of the constituent fermions. The interaction kernel is characterized by the matrices Γ^i , where $\Gamma^S = 1$, $\Gamma^V = \gamma^\mu$, $\Gamma^T = \sigma^{\mu\nu}$, $\Gamma^A = \gamma^\mu \gamma^5$, $\Gamma^P = \gamma^5$.

We now make the instantaneous approximation, so that the kernels $K^i = K^i(\mathbf{p} - \mathbf{q})$ in the rest frame. This reduces the Bethe-Salpeter equation to the Salpeter equation. It may seem like Lorentz invariance is lost by making this approximation. However, although manifest Lorentz invariance is lost, the Salpeter equation can be formulated covariantly by letting K^i depend on $q_\perp = q - \frac{q \cdot P}{M^2} P$ and $p_\perp = p - \frac{p \cdot P}{M^2} P$ in a general frame. In the rest frame q_\perp reduces to $(0, \mathbf{q})$. For details, see for example Chang and Chen [18].

It is most convenient to calculate the mass spectrum and wave functions in the rest frame of the bound states, and afterwards Lorentz transform the wave functions when needed. We will therefore perform the calculations in the rest frame for the remainder of the paper.

The propagators can be written

$$\begin{aligned}
\frac{1}{\not{q} - m} &= \left(\frac{\Lambda_+^+(\mathbf{q})}{(q^0 - E(\mathbf{q}) + i\epsilon)} + \frac{\Lambda_+^-(\mathbf{q})}{(q^0 + E(\mathbf{q}) - i\epsilon)} \right) \gamma^0 \\
&= \gamma^0 \left(\frac{\Lambda_+^-(\mathbf{q})}{(q^0 - E(\mathbf{q}) + i\epsilon)} + \frac{\Lambda_+^+(\mathbf{q})}{(q^0 + E(\mathbf{q}) - i\epsilon)} \right), \tag{2}
\end{aligned}$$

where

$$\Lambda_\mu^\pm(\mathbf{q}) = \frac{1}{2E(\mathbf{q})} (E(\mathbf{q}) + \mu(\pm\boldsymbol{\alpha} \cdot \mathbf{q} + m\gamma^0)) \quad \mu = \pm \tag{3}$$

are the projection operators for the positive and negative energy states respectively.

With the help of these projection operators we can write the Salpeter equation as a set of four coupled equations,

$$\begin{aligned}
\Lambda_\mu^+(\mathbf{q})\chi(q)\Lambda_\nu^-(\mathbf{q}) &= \frac{i}{(M/2 + q^0 - \mu E + \mu i\epsilon)(-M/2 + q^0 - \nu E + \nu i\epsilon)} \times \\
&\quad \sum_i \int \frac{d^4p}{(2\pi)^4} K^i(\mathbf{p} - \mathbf{q}) \Lambda_\mu^+(\mathbf{q}) \gamma^0 \Gamma^i \chi(p) \Gamma^i \gamma^0 \Lambda_\nu^-(\mathbf{q}). \tag{4}
\end{aligned}$$

The right hand side can be integrated over q^0 by a simple contour integration. Introducing the reduced wave function

$$\Psi(\mathbf{q}) = \int \frac{dq^0}{2\pi} \chi(q) \tag{5}$$

we find that

$$\Lambda_+^+(\mathbf{q})\Psi(\mathbf{q})\Lambda_-^-(\mathbf{q}) = -\frac{1}{(M - 2E)} \sum_i \int \frac{d\mathbf{p}}{(2\pi)^3} K^i(\mathbf{p} - \mathbf{q}) \Lambda_+^+(\mathbf{q}) \gamma^0 \Gamma^i \Psi(\mathbf{p}) \Gamma^i \gamma^0 \Lambda_-^-(\mathbf{q}), \tag{6}$$

$$\Lambda_-^+(\mathbf{q})\Psi(\mathbf{q})\Lambda_+^-(\mathbf{q}) = \frac{1}{(M + 2E)} \sum_i \int \frac{d\mathbf{p}}{(2\pi)^3} K^i(\mathbf{p} - \mathbf{q}) \Lambda_-^+(\mathbf{q}) \gamma^0 \Gamma^i \Psi(\mathbf{p}) \Gamma^i \gamma^0 \Lambda_+^-(\mathbf{q}), \tag{7}$$

$$\Lambda_+^+(\mathbf{q})\Psi(\mathbf{q})\Lambda_+^-(\mathbf{q}) = 0, \tag{8}$$

$$\Lambda_-^+(\mathbf{q})\Psi(\mathbf{q})\Lambda_-^-(\mathbf{q}) = 0. \tag{9}$$

Combining these equations with (4), we can write the wave function as

$$\begin{aligned}
\chi(q) &= \\
&= -\frac{i(M - 2E)}{(M/2 + q^0 - E + i\epsilon)(-M/2 + q^0 + E - i\epsilon)} \Lambda_+^+(\mathbf{q})\Psi(\mathbf{q})\Lambda_-^-(\mathbf{q}) \\
&\quad + \frac{i(M + 2E)}{(M/2 + q^0 + E - i\epsilon)(-M/2 + q^0 - E + i\epsilon)} \Lambda_-^+(\mathbf{q})\Psi(\mathbf{q})\Lambda_+^-(\mathbf{q}) \\
&\quad + \frac{i}{(M/2 + q^0 - E + i\epsilon)(-M/2 + q^0 - E + i\epsilon)} \int \frac{d\mathbf{p}}{(2\pi)^3} K^i \Lambda_+^+(\mathbf{q}) \gamma^0 \Gamma^i \Psi(\mathbf{p}) \Gamma^i \gamma^0 \Lambda_+^-(\mathbf{q}) \\
&\quad + \frac{i}{(M/2 + q^0 + E - i\epsilon)(-M/2 + q^0 + E - i\epsilon)} \int \frac{d\mathbf{p}}{(2\pi)^3} K^i \Lambda_-^+(\mathbf{q}) \gamma^0 \Gamma^i \Psi(\mathbf{p}) \Gamma^i \gamma^0 \Lambda_-^-(\mathbf{q}). \tag{10}
\end{aligned}$$

Thus, finding the wave function $\chi(q)$ in this formalism reduces to finding $\Psi(\mathbf{q})$.

Combining the equations (6)-(9) we get an equation for $\Psi(\mathbf{q})$,

$$\begin{aligned} & \left(\frac{M}{2} - \boldsymbol{\alpha} \cdot \mathbf{q} - m\gamma^0\right)\Psi(\mathbf{q}) + \Psi(\mathbf{q})\left(\frac{M}{2} - \boldsymbol{\alpha} \cdot \mathbf{q} + m\gamma^0\right) \\ &= -\sum_i \int \frac{d\mathbf{p}}{(2\pi)^3} K^i(\mathbf{p} - \mathbf{q}) (\Lambda_+^+(\mathbf{q})\gamma^0\Gamma^i\Psi(\mathbf{p})\Gamma^i\gamma^0\Lambda_-^-(\mathbf{q}) - \Lambda_-^+(\mathbf{q})\gamma^0\Gamma^i\Psi(\mathbf{p})\Gamma^i\gamma^0\Lambda_+^-(\mathbf{q})). \end{aligned} \quad (11)$$

For each state with a certain angular momentum, parity, and charge parity, we expand the function $\Psi(\mathbf{q})$ in the Dirac algebra by imposing the correct transformation properties. We also demand that $\Psi(\mathbf{q})$ fulfills the conditions (8)-(9). For example the expansion of the 0^{-+} state is

$$\Psi(\mathbf{q}) = \Psi_P(q)\gamma^5 + \Psi_A(q)\left(\gamma^0\gamma^5 + \gamma^5\frac{\boldsymbol{\alpha} \cdot \mathbf{q}}{m}\right). \quad (12)$$

The scalar functions Ψ_A and Ψ_P depend only on $q = |\mathbf{q}|$. Similar expansions for other states are given in Appendix A.

Integral equations for the scalar functions Ψ_i can be obtained from (11) by expanding both sides in the Dirac algebra and comparing the coefficients. This is discussed further in Appendix C, where all integral equations are given.

III. THE POTENTIAL

We have chosen a potential which consists of one short-range part describing the one-gluon-exchange interaction and one long-range confining part. The calculations have been done both in the Feynman gauge and in the Coulomb gauge, in an attempt to study the gauge dependence in the instantaneous approximation. The respective potentials are

$$K_{\text{Feyn}}(r) = K^V(r)\gamma_\mu^{(1)}\gamma^{\mu(2)} + K^S(r) + U, \quad (13)$$

$$K_{\text{Col}}(r) = K^V(r)\left(\gamma^{0(1)}\gamma^{0(2)} - \frac{1}{2}\boldsymbol{\gamma}^{(1)}\boldsymbol{\gamma}^{(2)} + \frac{1}{2}(\boldsymbol{\gamma}^{(1)} \cdot \hat{\mathbf{x}})(\boldsymbol{\gamma}^{(2)} \cdot \hat{\mathbf{x}})\right) + K^S(r) + U, \quad (14)$$

where U is a constant and

$$K^V(r) = \frac{\bar{\alpha}_s}{r}, \quad (15)$$

$$K^S(r) = \lambda r. \quad (16)$$

In momentum space the vector part in the Coulomb gauge becomes

$$\frac{4\pi\bar{\alpha}_s}{(\mathbf{p} - \mathbf{q})^2} \left(\gamma_\mu^{(1)}\gamma^{\mu(2)} + (\boldsymbol{\gamma}^{(1)} \cdot (\hat{\mathbf{p}} - \hat{\mathbf{q}}))(\boldsymbol{\gamma}^{(2)} \cdot (\hat{\mathbf{p}} - \hat{\mathbf{q}}))\right) \quad (17)$$

The color factor $4/3$ is included in $\bar{\alpha}_s$, $\bar{\alpha}_s = 4/3\alpha_s$. We let the coupling be constant, since a running coupling would not make any significant difference for heavy mesons like charmonium.

There are four parameters in the model: $\bar{\alpha}_s$, λ , U , and the quark mass m . These will be determined by a least square fit to the mass spectrum and the ratios of the lepton pair decays.

Olsson *et al.* [10] have recently investigated the stability of the Salpeter equation for various Lorentz structures of the confining kernel. They have come to the conclusion that for light and medium-heavy quarks numerically stable solutions exist only for a time component vector potential. The same result has also been found by Parramore and Piekarewicz [11,12] from a similar analysis.

However, we have found no such problems for heavy quarks like in the charmonium system. This has also been confirmed in Ref. [5]. Furthermore, a time component vector confinement gives a contribution to the spin-orbit coupling with the wrong sign, which speaks in favor of a scalar confinement.

We want to be able to perform the angular integrations in the Salpeter equation analytically. We therefore need the expansions of the potential in spherical harmonics in momentum space as

$$K^i(\mathbf{p} - \mathbf{q}) = \sum_{\ell m} F_\ell^i(p, q) Y_{\ell m}^*(\hat{\mathbf{p}}) Y_{\ell m}(\hat{\mathbf{q}}), \quad i = V, S. \quad (18)$$

The expansion of the Coulomb potential is

$$K^V(\mathbf{p} - \mathbf{q}) = \frac{4\pi\bar{\alpha}_s}{(\mathbf{p} - \mathbf{q})^2} = \frac{8\pi^2\bar{\alpha}_s}{pq} \sum_{\ell m} Q_\ell \left(\frac{p^2 + q^2}{2pq} \right) Y_{\ell m}^*(\hat{\mathbf{p}}) Y_{\ell m}(\hat{\mathbf{q}}), \quad (19)$$

where Q_ℓ are the Legendre functions of second kind. Thus

$$F_\ell^V(p, q) = \frac{8\pi^2\bar{\alpha}_s}{pq} Q_\ell \left(\frac{p^2 + q^2}{2pq} \right). \quad (20)$$

In the Coulomb gauge potential (17) there is another angular dependence in the second term. However, we later choose to give this dependence in terms of the functions F_ℓ^V .

The Fourier transform of the linear potential can only be defined in a distributional sense. This causes no problems as in momentum space the value of the potential at each point is not important, but only its action on a wave function. We define $K^S(r)$ as the limit

$$K^S(r) = \lim_{\epsilon \rightarrow 0} \frac{\partial^2}{\partial \epsilon^2} \left(\frac{\lambda e^{-\epsilon r}}{r} \right). \quad (21)$$

This gives

$$\begin{aligned} K^S(\mathbf{p} - \mathbf{q}) &= \lim_{\epsilon \rightarrow 0} \frac{\partial^2}{\partial \epsilon^2} \left(\frac{4\pi\lambda}{(\mathbf{p} - \mathbf{q})^2 + \epsilon^2} \right) \\ &= \lim_{\epsilon \rightarrow 0} \frac{8\pi^2\lambda}{pq} \sum_{\ell m} \frac{\partial^2}{\partial \epsilon^2} Q_\ell \left(\frac{p^2 + q^2 + \epsilon^2}{2pq} \right) Y_{\ell m}^*(\hat{\mathbf{p}}) Y_{\ell m}(\hat{\mathbf{q}}). \end{aligned} \quad (22)$$

It can be shown [19], that in a distributional sense, the following relation holds:

$$\begin{aligned} &\lim_{\epsilon \rightarrow 0} \int_0^\infty dp \frac{\partial^2}{\partial \epsilon^2} Q_\ell \left(\frac{p^2 + q^2 + \epsilon^2}{2pq} \right) f(p) \\ &= \text{PV} \int_0^\infty dp \left(\frac{1}{pq} Q'_\ell \left(\frac{p^2 + q^2}{2pq} \right) f(p) + \frac{4q^2}{(p+q)^2(p-q)^2} f(q) \right), \end{aligned} \quad (23)$$

where PV means the principal value. Thus

$$\begin{aligned} & \int_0^\infty \frac{dp}{(2\pi)^3} p^2 F_\ell^S(p, q) \Psi(p) \\ &= \text{PV} \int_0^\infty \frac{dp}{(2\pi)^3} 8\pi^2 \lambda \left(\frac{1}{q^2} Q'_\ell \left(\frac{p^2 + q^2}{2pq} \right) \Psi(p) + \frac{4q^2}{(p+q)^2(p-q)^2} \Psi(q) \right). \end{aligned} \quad (24)$$

IV. LEPTON PAIR DECAYS

We now continue with a discussion of the decay observables. A general prescription for calculating matrix elements of the electromagnetic current operator between bound states has been given by Mandelstam [17]. We begin with the lepton pair decays, which we will use together with the mass spectrum, in order to optimize the four parameters $\bar{\alpha}_s$, λ , U , and m in the model. The probability for a vector particle decaying into two light leptons is

$$\Gamma = \frac{4\pi\alpha^2 e_q^2}{M^3} |j^\mu j_\mu|^2, \quad (25)$$

where j^μ is the vector quark current, e_q is the charge of the quark, and M is the mass of the vector particle. To lowest order in the electromagnetic coupling the current is, in the rest frame of the decaying particle,

$$j^\mu = -\text{Tr} \int \frac{d^4q}{(2\pi)^4} \gamma^\mu \chi(q) = -\text{Tr} \int \frac{d\mathbf{q}}{(2\pi)^3} \gamma^\mu \Psi(\mathbf{q}). \quad (26)$$

The corresponding Feynman diagram is given in Fig. 1.

Taking the trace we find that $j^0 = 0$ (whence the current is conserved) and

$$\mathbf{j} = \int \frac{d\mathbf{q}}{(2\pi)^3} \left(\frac{4m}{q^2} \mathbf{q} \Psi_S(q) Y_{1m}(\hat{\mathbf{q}}) + 4\Psi_V(q) \mathbf{Y}_{1m}^{(e)}(\hat{\mathbf{q}}) \right). \quad (27)$$

We have here used the expansion (A2) of the 1^{--} state given in Appendix A.

Performing the angular integration we get

$$|\mathbf{j}|^2 = \left(\int \frac{dq}{(2\pi)^3} \left(8mq \sqrt{\frac{\pi}{3}} \Psi_S(q) + 8q^2 \sqrt{\frac{2\pi}{3}} \Psi_V(q) \right) \right)^2. \quad (28)$$

The expression for the leptonic decay is divergent and has to be renormalized [20]. This can in principle be done in several ways. However, here we must take into account the fact that the theory is not fully defined. This means that with an interaction kernel which is instantaneous and defined by the ladder expansion only, the Ward-Takahashi identities are not appropriate. The divergence of the wavefunction at the origin can therefore only be related to the (experimental) value of the vertex function at some suitable momentum transfer. For non-confining potentials, such as the Coulomb potential, there is a region of production of asymptotically free fermions above threshold. The production cross section

can then be calculated with the kernel and the result be taken as a measure of the vertex function. This is more or less the choice in Ref. [20]. In our case the potential is confining and consists of two parts, one of which has a dimensionful coupling constant λ . This means that the renormalization has to be done in the deep inelastic region, where the quarks are asymptotically free and the linear part of the potential is negligible. This presents several problems since the lack of manifest covariance makes the renormalization constant depend upon both the cut-off and the momentum.

The problem appears as follows. We would like to define a renormalization constant Z_1 , such that

$$\lim_{\Lambda \rightarrow \infty} Z_1(\Lambda) \int^\Lambda d\mathbf{q} \gamma^\mu \Psi(\mathbf{q}) = \text{finite}. \quad (29)$$

Asymptotically $\Psi(\mathbf{q}) \sim q^{-3+\beta}$, and thus $j^\mu \sim \Lambda^\beta$ for large Λ , where β is determined from the dynamics [20].

The renormalization constant, Z_1 , is defined through the (analytically continued) vertex function Γ^μ by

$$\bar{u}(\mathbf{q})\Gamma^\mu u(\mathbf{q}) = Z_1^{-1}(q)\bar{u}(\mathbf{q})\gamma^\mu u(\mathbf{q}) \quad (30)$$

and the vertex function satisfies

$$\begin{aligned} \Gamma(\mathbf{q}) = & \gamma + i \int^\Lambda \frac{d^4 p}{(2\pi)^4} K^V(\mathbf{p} - \mathbf{q}) \gamma^\mu \frac{1}{\not{p} - m} \Gamma(\mathbf{p}) \frac{1}{\not{p} - m} \gamma_\mu \\ & + i \int^\Lambda \frac{d^4 p}{(2\pi)^4} K^S(\mathbf{p} - \mathbf{q}) \frac{1}{\not{p} - m} \Gamma(\mathbf{p}) \frac{1}{\not{p} - m}. \end{aligned} \quad (31)$$

The renormalization constant Z_1 has the correct asymptotic behavior to cancel the Λ -dependence of the current. However, due to the instantaneous approximation, Z_1 depends on q . With only a Coulomb potential, Z_1 has the correct Λ -dependence to cancel the divergence of j^μ as $\Lambda \rightarrow \infty$ for any momentum q . However, with a confining part added to the potential this would only be true in the region $q \rightarrow \infty$, where the linear potential is negligible. Unfortunately, $Z_1 \sim q^\beta$ when $q \rightarrow \infty$, and therefore the theory is not renormalizable in this way.

The electromagnetic theory can only be used in lowest order due to the non-existence of Ward-Takahashi identities in the instantaneous approximation since the theory is not fully defined. Nevertheless there is a loop contribution in the current j^μ which has to be renormalized. As the vertex function cannot be renormalized, we therefore adopt the philosophy that, for confining potentials, the most natural experimental datum at which to fix the normalization is the resonance formation itself. The renormalization should therefore be effected by using, say, the decay width for the lowest resonance as input. The other decay widths are then calculated relative to this. Thus we will optimize only the ratios of the decay constants for successive nS states as predictable by the model. These ratios are independent of the cut-off Λ for $\Lambda \geq 30$ GeV to within 1%.

Another way to avoid the problem with infinities would be to redefine the potential to take a finite value for $r = 0$. This would make the current (27) finite. However, the theory must still be renormalized although only a finite renormalization is necessary in this case.

Therefore such an approach would still face the same problem as explained above, as a new dimensionful constant must be introduced in the cut-off of the potential. Our opinion is that our approach is much cleaner and conceptually more transparent.

V. $\gamma\gamma$ DECAYS

The calculation of the $\gamma\gamma$ decays is most easily performed in the rest frame of the bound state, which decays into two photons with momenta $k_1 = (M/2, \mathbf{k})$ and $k_2 = (M/2, -\mathbf{k})$. To lowest order the matrix element is given by

$$\begin{aligned} M^{\mu\nu} &= \text{Tr} \int \frac{d^4q}{(2\pi)^4} \chi(q) \left(\gamma^\mu \frac{1}{\not{P}/2 + \not{q} - \not{k}_1 - m} \gamma^\nu + \gamma^\nu \frac{1}{\not{P}/2 + \not{q} - \not{k}_2 - m} \gamma^\mu \right) \\ &= \text{Tr} \int \frac{d^4q}{(2\pi)^4} \chi(q) \left(\gamma^\mu \frac{1}{\not{q} + \boldsymbol{\gamma} \cdot \mathbf{k} - m} \gamma^\nu + \gamma^\nu \frac{1}{\not{q} - \boldsymbol{\gamma} \cdot \mathbf{k} - m} \gamma^\mu \right). \end{aligned} \quad (32)$$

The corresponding Feynman diagrams are given in Fig. 2. The decay probability is given by

$$\Gamma = \frac{3\pi\alpha^2 e_q^4}{2(2J+1)M} \sum |\epsilon_1^\mu \epsilon_2^\nu M_{\mu\nu}|^2, \quad (33)$$

where e_q is the charge of the quark, and M is the meson mass and J its angular momentum.

The amplitude $\epsilon_1^\mu \epsilon_2^\nu M_{\mu\nu}$ can be expressed in the scalar amplitudes for the different decaying states. This is discussed in Appendix E.

VI. M1 AND E1 TRANSITIONS

In the rest frame of the initial particle the matrix element for the M1 and E1 transitions is, in the ladder approximation, given by

$$\begin{aligned} M^\mu &= \text{Tr} \int \frac{d^4q}{(2\pi)^4} \bar{\chi}_f(q - k/2, P_f) \gamma^\mu \chi_i(q, M_i) \left(-\frac{M_i}{2} \gamma^0 + \not{q} - m \right) \\ &\quad + \text{Tr} \int \frac{d^4q}{(2\pi)^4} \bar{\chi}_f(q + k/2, P_f) \left(\frac{M_i}{2} \gamma^0 + \not{q} - m \right) \chi_i(q, M_i) \gamma^\mu. \end{aligned} \quad (34)$$

Here $\chi_i(q, M_i)$ is the wave function of the initial particle in its rest frame, and $\bar{\chi}_f(q \pm k/2, P_f)$ is the wave function of the final particle in a frame where it moves with momentum P_f . This wave function is found by Lorentz transforming the one in the rest frame, see Appendix D 1. The Feynman diagrams corresponding to M^μ are given in Fig. 3.

The decay probability is given by

$$\Gamma = \frac{\alpha e_q^2 k}{2M_i^2 (2J+1)} \sum |\epsilon_\mu M^\mu|^2, \quad (35)$$

where e_q is the charge of the quark, k the photon momentum, M_i the mass of the initial meson and J its angular momentum.

To calculate the matrix element we use the expansions of the wave functions given in Appendix D. We first perform the q^0 integration. Since the Lorentz transformed state $\chi(q - k/2, P_f)$ has a very complicated analytic structure we cannot make a simple contour integration. We have to use the principal value technique. The real part is given by a sum of residues

$$\text{Re } i \int dq^0 \frac{f(q^0)}{g(q^0) \pm i\epsilon} = \pm \pi \frac{f(p_k^0)}{|g'(p_k^0)|}, \quad (36)$$

where p_k^0 is a zero of $g(p^0)$. The imaginary part gives an unphysical non-Hermitian contribution to the decay width. It should vanish in any consistent covariant theory, but in the Salpeter model it has been verified that it does not vanish [6], because of the lack of manifest covariance. However, for the charmonium system this unphysical contribution is negligible, and we therefore neglect it.

The integration over the azimuthal angle φ can also be done analytically. The rest of the calculation is made numerically. Trying to take the trace analytically creates enormously complicated expressions which are hardly of any use.

A. Gauge invariance of the matrix element

In a Bethe-Salpeter model without the instantaneous approximation where we have an even kernel of the form $K(p - q)$, the gauge invariance of the matrix element can be shown with the help of the Bethe-Salpeter equation. Let the initial meson have momentum P_i and the final meson have momentum $P_f = P_i - k$, where k is the photon momentum. Then

$$\begin{aligned} k_\mu M^\mu &= \int \frac{d^4q}{(2\pi)^4} \bar{\chi}(q - k/2, P_f) \not{k} \chi(q, P_i) \left(-\frac{P_i}{2} + \not{q} - m\right) \\ &= \int \frac{d^4q}{(2\pi)^4} \bar{\chi}(q - k/2, P_f) \left(\frac{P_i}{2} + \not{q} - m\right) \chi(q, P_i) \left(-\frac{P_i}{2} + \not{q} - m\right) \\ &\quad - \int \frac{d^4q}{(2\pi)^4} \bar{\chi}(q - k/2, P_f) \left(\frac{P_f}{2} + \not{q} - \frac{\not{k}}{2} - m\right) \chi(q, P_i) \left(-\frac{P_f}{2} + \not{q} - \frac{\not{k}}{2} - m\right) \\ &= \int \frac{d^4q}{(2\pi)^4} \frac{d^4p}{(2\pi)^4} \bar{\chi}(q - k/2, P_f) K(q - p) \chi(p, P_i) \\ &\quad - \int \frac{d^4q}{(2\pi)^4} \frac{d^4p}{(2\pi)^4} \bar{\chi}(p, P_f) K(q - k/2 - p) \chi(q, P_i) \\ &= \int \frac{d^4q}{(2\pi)^4} \frac{d^4p}{(2\pi)^4} \bar{\chi}(q - k/2, P_f) K(q - p) \chi(p, P_i) \\ &\quad - \int \frac{d^4q}{(2\pi)^4} \frac{d^4p}{(2\pi)^4} \bar{\chi}(p - k/2, P_f) K(q - p) \chi(q, P_i) = 0 \end{aligned} \quad (37)$$

provided the order of integrations can be interchanged. This proves gauge invariance.

However, if the kernel depends on the momentum of the bound state, as it does in the instantaneous approximation, the terms in the last line do not cancel. In the first term K depends on P_i , and in the second term on P_f .

Nevertheless, in the instantaneous approximation we have verified that $\mathbf{k} \cdot \mathbf{M} = 0$ and $M^0 = 0$ in the rest frame of the decaying particle, by performing the angular integration of the decay amplitude. Thus gauge invariance is fulfilled.

VII. NUMERICAL RESULTS

The eigenvalue equations given in Appendix C were solved numerically by expanding the wave function in cubic Hermite splines [21]. However, first the integration region $0 \leq p < \infty$ was transformed into the finite interval $-1 \leq x \leq 1$ by $x = (p - p_0)/(p + p_0)$, where p_0 was chosen in the physically relevant region. The integration and the following matrix eigenvalue problem for the expansion coefficients were solved with standard methods. We have tested the stability of the solutions by varying the number of basis functions and the parameter p_0 , and found that the eigenvalues do not change. Problems, like the ones reported in Refs. [10–12] for lighter quarks, have not been seen.

The parameters $\bar{\alpha}_s$, m , λ , and U of the model are determined by making a least square fit to the mass spectrum and the ratios of the lepton pair decay widths $J/\Psi/\Psi(2S)$ and $\Psi(2S)/\Psi(3S)$. As discussed in Sec. IV we renormalize the decay widths to the experimental value of the decay of J/Ψ . We therefore make the fit to the ratios between the widths rather than the widths themselves. We minimize the function

$$\chi^2 = \sum \frac{(M_i(\text{theory}) - M_i(\text{exp}))^2}{\sigma_i^2} + \sum \frac{(\Gamma_i(\text{theory})/\Gamma_j(\text{theory}) - \Gamma_i(\text{exp})/\Gamma_j(\text{exp}))^2}{\sigma_{i/j}^2}. \quad (38)$$

The first sum goes over all the charmonium masses in Table I except $\eta_c(2S)$ and h_{c1} which are not used in the fit because they still need experimental confirmation. The second sum is over the two ratios of lepton pair decay widths $\Gamma(J/\Psi)/\Gamma(\Psi(2S))$ and $\Gamma(\Psi(2S))/\Gamma(\Psi(3S))$. We have not used the decay widths for the higher states because their wave functions are not good enough to be used for calculations of decay widths. The experimental errors for the ratios, $\sigma_{i/j}$, are numerically $\sigma_{J/\Psi/2S} = 0.30$ and $\sigma_{2S/3S} = 0.64$ respectively.

As many of the masses are very accurately measured, using the true experimental error for the masses in this function would make the masses totally dominate over the decay width. We therefore use a minimum value of σ_i when the experimental error is small. Two fits for both gauges have been made, one where we have used $\sigma_i = 10$ MeV for the masses when the experimental error is smaller than 10 MeV, and one where we have used $\sigma_i = 50$ MeV for the masses when the experimental error is smaller than 50 MeV. We use the true experimental errors for $\sigma_{i/j}$ in both fits. In the second fit we thus give the lepton decays a higher weight, though in both cases the masses get a higher weight than the decay widths as the errors of the decay widths are rather large. The numerical results of the four fits can be found in Tables I and II. In these tables F and C stand for Feynman and Coulomb gauge respectively, and 10 and 50 MeV stand for the minimum value of σ_i .

Making four fits gives us a chance to see how sensitive the different decay observables are to changes of the model parameters. The parameter values in the four different cases can be found in Table III. We see that when we change σ_i from 10 MeV to 50 MeV the parameter which changes most is the constant U . One would perhaps expect that $\bar{\alpha}_s$ would be the parameter most sensitive to such a change in σ_i , as the lepton pair decays should be very

sensitive to $\bar{\alpha}_s$ because they depend on the value of the wavefunction at the origin. However, we calculate the ratios between the decay widths rather than the widths themselves, and these ratios are not very sensitive to the value of $\bar{\alpha}_s$. This can be understood by noting that in a non-relativistic model with a Coulomb potential the ratios of the wave functions' value at the origin are independent of the coupling constant. On the other hand, $\bar{\alpha}_s$ of course changes a lot between the fits in the two different gauges to compensate for the differences in the structure of the vector part of the potential, while the other parameters remain almost constant.

The bottom row in Table I shows the total χ^2 for the four fits. A fictitious error of 10 MeV for all masses has been used to calculate the values in order to make them comparable. We see that we obtain a slightly better result in the Coulomb gauge and that in the Feynman gauge we obtain the largest difference between the fits with different σ_i .

In Table II the χ^2 values in the row just above the lepton pair decays measure the quality of the calculation of the E1, M1, and two gamma transitions. We have here excluded the decay $\Psi(2S) \rightarrow \eta_c \gamma$ as it would totally dominate χ^2 . We see that the results in the Coulomb gauge changes most and that the Feynman gauge on average gives a better result although the Coulomb gauge with $\sigma_i = 50$ MeV is better than any of the two fits in Feynman gauge.

In the last row in the same table we find the χ^2 values for the lepton pair decays. The decays of the D states have been excluded in the calculation as they depend on higher order corrections not included in our calculations. We see that the Feynman gauge clearly gives a better result.

In conclusion the Coulomb gauge gives better results for the masses, the Feynman gauge gives better results for the lepton pair decays and the results for the two gamma, E1, and M1 transitions are fairly equal, perhaps slightly better in Feynman gauge. The overall differences are not so large that we can clearly tell which one of the two gauges gives best results.

The lepton decay widths are normalized such that the value for J/Ψ agrees with the experimental value. We see that the other values for the S states become too large. This indicates that we lack a fine-tuning of the shape of the potential. A smaller slope of the linear confinement potential would push the wave function further away from the origin but would on the other hand make the mass spectrum worse. That the decay widths for the D states are rather small is not surprising, as they mainly come from higher order corrections not included here. In non-relativistic models with a Coulomb potential the wave function for D states is zero at the origin, which give a vanishing decay width. In the Salpeter model this means that higher order corrections to the kernel in the ladder approximation are very important for the D states.

The values for the two gamma decays agree very well with experiment, and the values for the E1 transitions agree fairly well although the values for the decays including the χ_{c1} state all come out about a factor of two too large.

When it comes to the M1 transitions we see that the predicted value of the $J/\Psi \rightarrow \gamma \eta_c$ decay width agrees very well with experimental data. On the other hand the $\Psi(2S)$ decay width is far too large. This is because the wave function of the excited state is not determined well enough, and as this decay is forbidden it is extremely sensitive to the exact shape of the wave functions.

For light quarks, the non-relativistic quark model parameters usually relate the magnetic

moments directly to the constituent masses and there is no room in the parameterization, so to speak, to introduce anomalous magnetic moments.

For the charm quark the current and constituent masses should be essentially the same and there is then a possibility to introduce an anomalous magnetic moment as a new independent parameter.

The details of the decay mechanism are in principle sensitive to this parameter. In the absence so far of any measurement of the magnetic moment of charmed baryons, the radiative decay rates therefore constitute at present the only place where this parameter can be studied.

Once an accurate determination of the wave functions can be made, the anomalous magnetic moment can be calculated from the M1 transitions. But it is important to notice that the outcome of such a calculation depends heavily on the quark mass. Therefore a determination of the quark mass must be made first. An estimate of the anomalous magnetic moment have previously been made in a Salpeter model where a non-relativistic approximation has been made [22].

A calculation of lepton pair decays and E1 transitions has earlier been done by Ito [15] in a model where only the positive energy term is used in the Salpeter equation. Recently a calculation of all decay observables has been done by Resag et al. [5] in a Salpeter model, but with a cut-off in the potential to regularize the divergence in the lepton pair decay amplitude. The overall results in both these calculations are of about the same quality as in ours. As we have discussed earlier, the lepton pair decays depend of the cut-off parameter, and therefore have to be renormalized before they can be compared. Doing so, we see that their results for a scalar confinement are almost identical with our results in Feynman gauge with $\sigma_i = 10$ MeV.

VIII. IMPORTANCE OF NON-DOMINANT TERMS

Sometimes the Salpeter equation is reduced to only the term with the positive energy states of the quark. This is done by making the following replacement of the propagators (2) in the Salpeter equation:

$$\frac{1}{\not{q} - m} \longrightarrow \frac{\Lambda_+^+(\mathbf{q})\gamma^0}{(q^0 - E(\mathbf{q}) + i\epsilon)} = \frac{\gamma^0\Lambda_-^-(\mathbf{q})}{(q^0 + E(\mathbf{q}) - i\epsilon)} \quad (39)$$

This imposes an extra constraint on the reduced wave function $\Psi(\mathbf{q})$. Eq. (7) is replaced by

$$\Lambda_-^+(\mathbf{q})\Psi(\mathbf{q})\Lambda_+^-(\mathbf{q}) = 0 \quad (40)$$

For the wave function $\chi(q)$ only the first term in (10) remains:

$$\chi(q) = -\frac{i(M - 2E)}{(M/2 + q^0 - E + i\epsilon)(-M/2 + q^0 + E - i\epsilon)}\Lambda_+^+(\mathbf{q})\Psi(\mathbf{q})\Lambda_-^-(\mathbf{q}) \quad (41)$$

Does this reduction change the results significantly? Olsson *et al.* [13] have recently investigated the validity of the reduced Salpeter equation by comparing the eigenvalues and wave functions found from the full and reduced Salpeter equation. They found that there is

only a significant difference for light quarks, and for as heavy ones as the charm quark the difference is very small.

However, this does not completely test the validity of the reduced Salpeter equation. In particular this does not tell us how important the last two terms in (10) are. They do not appear in the calculation of the mass spectrum, which only involves the reduced wave function $\Psi(\mathbf{q})$. On the other hand, the E1 and M1 transitions do include these two terms.

To test the validity of the reduced Salpeter equation we have therefore compared the decay widths for E1 and M1 transitions using only the terms with positive energy states and the widths using all terms. We have not solved the reduced Salpeter equation but only neglected all but the dominant term. This will not give us an exact comparison with the reduced Salpeter equation but as have been shown by Olsson *et al.* [13] the wave functions differ very little. The result is shown in Table IV. We see that the decay widths change considerably if we neglect all but the dominant term, in some cases with more than 100 %. This shows the importance of keeping all terms. Although the magnitude of the negative energy part of the reduced wave functions is small – the contribution to the norm is typically $< 5\%$ – there are other terms in the decay amplitudes which make the contribution from the non-dominant terms significant.

This can be understood if we note that the last two terms in the wave function (10) do not appear in the expression for the norm (B6). Using the reduced Salpeter equation leads to a normalization condition with only the first term in (B6). The omitted second term is small and thus changes the normalization very little.

To further illustrate this we have plotted the functions

$$\frac{m}{E(q)}\Psi_P(q) \pm \Psi_A(q)$$

and

$$\frac{I_0(q)}{E(q)}$$

for the 0^{-+} state in Fig. 4. These functions appears in the amplitudes of 0^{+-} 's wave function. We see that negative energy amplitude $\frac{m}{E(q)}\Psi_P(q) - \Psi_A(q)$ is considerably smaller than the positive energy amplitude. The amplitude I_0/E appearing in the last two terms of the wave function (10) is somewhere in between in magnitude. However, it should be noted that it is difficult to directly compare this function to the other two because of the other factors in the amplitudes coming from the propagators. But we see that it is clearly not negligible.

Comparing the mass spectrum and wave functions is therefore not enough to tell if an approximation is valid. The decay widths must also be studied. Using the reduced Salpeter equation means that several terms in the decay widths are omitted and we have shown that these terms are very important in the E1 and M1 transitions. We conclude that the reduced Salpeter equation gives approximately the same result as the full Salpeter equations only for those quantities which do not depend on the last two terms in the wave function (10).

IX. SUMMARY AND CONCLUSIONS

We have done a thorough analysis of the charmonium system in a Salpeter model with an instantaneous potential. We have presented general equations for calculating the mass spectrum as well as decay widths for lepton pair decays, two gamma decays, M1 and E1 transitions. This has been done for a vector plus scalar potential both in the Coulomb and Feynman gauges. The formalism used is based on the one developed by Suttorp [1].

We have discussed the problem with the renormalization of the lepton pair decay amplitude in the instantaneous approximation. This approximation makes the renormalization constant Z_1 depend on q and $Z_1 \rightarrow \infty$ as $q \rightarrow \infty$. With a linear confining potential we have to make the renormalization in the region where the quarks are asymptotically free and the linear potential is negligible. But since $Z_1 \rightarrow \infty$ this leads to an inconsistency, and therefore the only natural way to define the renormalization constant is to normalize the calculated widths to the experimental value of the width $J/\Psi \rightarrow e^+e^-$.

Numerically we have obtained an excellent fit to the mass spectrum of charmonium. Most of the decay widths agree rather well with experiments, although the lepton pair decays of the excited S states are too large. The excited states are obviously more sensitive to fine-tuning of the model. A smaller slope of the linear confinement potential would push the wave function further away from the origin but would on the other hand make the mass spectrum worse. Similarly the poor result for the forbidden M1 transition $\Psi(2S) \rightarrow \eta_c \gamma$ indicates a lack of fine-tuning of the potential. We conclude that before any detailed predictions can be made from the Salpeter equation, a systematic way to improve the kernel must be developed.

Comparing the two gauges, Feynman and Coulomb gauge, we have found that the Coulomb gauge gives better results for the mass spectrum and that the Feynman gauge gives better results for the lepton pair decays. The overall difference is not large enough to clearly tell which gauge gives the best results.

The validity of the reduced Salpeter equation has been tested, and it has been found that the decay widths of the E1 and M1 transitions change considerably if one uses the reduced equation.

ACKNOWLEDGMENTS

This work was supported by the Swedish Natural Science Research Council (NFR), contract F-AA/FU03281-308.

APPENDIX A: WAVE FUNCTIONS FOR DIFFERENT STATES

We here present the expansion in the Dirac algebra of the reduced wave functions, $\Psi(\mathbf{q})$, defined in (5), for different states. These expansions are the most general ones with the correct transformation properties regarding angular momentum, parity, and charge parity, which also fulfill the conditions (8-9). All scalar functions Ψ_i depend only on $q = |\mathbf{q}|$.

$$0^{-+} : \quad \Psi(\mathbf{q}) = \left(\Psi_P(q)\gamma^5 + \Psi_A(q) \left(\gamma^0\gamma^5 + \gamma^5 \frac{\boldsymbol{\alpha} \cdot \mathbf{q}}{m} \right) \right) Y_{00}(\hat{\mathbf{q}}), \quad (\text{A1})$$

$$\begin{aligned}
1^{--} : \quad \Psi(\mathbf{q}) = & \left(\Psi_S(q) \left(1 + \frac{m}{q^2} \boldsymbol{\gamma} \cdot \mathbf{q} \right) + \Psi_{T_1}(q) \frac{\boldsymbol{\alpha} \cdot \mathbf{q}}{q} \right) Y_{1m}(\hat{\mathbf{q}}) \\
& + \left(\Psi_V(q) \boldsymbol{\gamma} + \Psi_{T_2}(q) \left(\boldsymbol{\alpha} - i\gamma^5 \frac{\mathbf{q} \times \boldsymbol{\gamma}}{m} \right) \right) \cdot \mathbf{Y}_{1m}^{(e)}(\hat{\mathbf{q}}), \tag{A2}
\end{aligned}$$

$$1^{+-} : \quad \Psi(\mathbf{q}) = \left(\Psi_P(q) \gamma^5 + \Psi_A(q) \left(\gamma^0 \gamma^5 + \gamma^5 \frac{\boldsymbol{\alpha} \cdot \mathbf{q}}{m} \right) \right) Y_{1m}(\hat{\mathbf{q}}), \tag{A3}$$

$$0^{++} : \quad \Psi(\mathbf{q}) = \left(\Psi_S(q) \left(1 + \frac{m}{q^2} \boldsymbol{\gamma} \cdot \mathbf{q} \right) + \Psi_T(q) \frac{\boldsymbol{\alpha} \cdot \mathbf{q}}{q} \right) Y_{00}(\hat{\mathbf{q}}), \tag{A4}$$

$$1^{++} : \quad \Psi(q) = \left(\Psi_V(q) i \frac{(\mathbf{q} \times \boldsymbol{\gamma})}{q} + \Psi_T(q) \left(i \frac{(\boldsymbol{\alpha} \times \mathbf{q})}{q} + \frac{q}{m} \gamma^5 \boldsymbol{\gamma} \right) \right) \cdot \mathbf{Y}_{1m}^{(e)}(\hat{\mathbf{q}}), \tag{A5}$$

$$\begin{aligned}
2^{++} : \quad \Psi(\mathbf{q}) = & \left(\Psi_S(q) \left(1 + \frac{m}{q^2} \boldsymbol{\gamma} \cdot \mathbf{q} \right) + \Psi_{T_1}(q) \frac{\boldsymbol{\alpha} \cdot \mathbf{q}}{q} \right) Y_{2m}(\hat{\mathbf{q}}) \\
& + \left(\Psi_V(q) \boldsymbol{\gamma} + \Psi_{T_2}(q) \left(\boldsymbol{\alpha} - i\gamma^5 \frac{\mathbf{q} \times \boldsymbol{\gamma}}{m} \right) \right) \cdot \mathbf{Y}_{2m}^{(e)}(\hat{\mathbf{q}}). \tag{A6}
\end{aligned}$$

Here the $Y_{\ell m}(\hat{\mathbf{q}})$'s are the scalar spherical harmonics and the $\mathbf{Y}_{\ell m}^{(e)}(\hat{\mathbf{q}})$'s are the electric vector spherical harmonics. The latter are defined in terms of the vector spherical harmonics,

$$\mathbf{Y}_{JL}^m = \sum_{m_1 m_2} Y_{Lm_1} \mathbf{e}_{m_2} (Lm_1 \ 1m_2 | Jm), \tag{A7}$$

where $\mathbf{e}_{\pm} = \mp(\mathbf{e}_x \pm i\mathbf{e}_y)/\sqrt{2}$ and $\mathbf{e}_0 = \mathbf{e}_z$, as

$$\mathbf{Y}_{Jm}^{(e)} = \sqrt{\frac{J+1}{2J+1}} \mathbf{Y}_{J,J-1}^m + \sqrt{\frac{J}{2J+1}} \mathbf{Y}_{J,J+1}^m. \tag{A8}$$

APPENDIX B: NORMALIZATION CONDITION

The wave functions satisfy the normalization condition [23]

$$\text{Tr} \int \frac{d^4 p}{(2\pi)^4} \int \frac{d^4 q}{(2\pi)^4} \bar{\chi}(p) P^\mu \frac{d}{dP^\mu} (I(p, q, P) + iK(p, q, P)) \chi(q) = 2iM^2, \tag{B1}$$

where

$$I(p, q, P) = (2\pi)^4 \delta^{(4)}(p - q) S_1^{-1}(P/2 + p) S_2^{-1}(-P/2 + p). \tag{B2}$$

The adjoint wave function $\bar{\chi}$ is defined

$$\bar{\chi} = \gamma^0 \chi^\dagger \gamma^0. \tag{B3}$$

We have contracted with P^μ in (B1). This is possible if the Salpeter equation is written in a covariant form. This is done by letting the kernel depend on the four-vectors $(0, \mathbf{q})$ and $(0, \mathbf{p})$ in the rest frame. The Salpeter equation is then Lorentz transformed by first multiplying it by the spinor transformation matrices $S(\Lambda)$ and $S^{-1}(\Lambda)$ from each side. Then

the change of variables $q \rightarrow \Lambda^{-1}q$ is made. The kernel is found to depend on the orthogonal part of the momentum $q_{\perp} = q - \frac{qP}{M^2}$ and $p_{\perp} = p - \frac{pP}{M^2}$ in a frame where the particle moves with momentum P . In the rest frame q_{\perp} reduces to $(0, \mathbf{q})$. Thus $K = K(q_{\perp} - p_{\perp})$. For such kernels we have

$$P^{\mu} \frac{d}{dP^{\mu}} K(q_{\perp} - p_{\perp}) = 0. \quad (\text{B4})$$

Thus the second term in (B1) does not contribute to the normalization. Integrating the other term over p gives the following normalization condition in the rest frame,

$$\text{Tr} \int \frac{d^4q}{(2\pi)^4} \bar{\chi}(q) \gamma^0 \chi(q) \left(-\frac{M}{2} \gamma^0 + \not{q} - m\right) = 2iM. \quad (\text{B5})$$

Using the form (10) of the wave function and integrating over q^0 gives

$$\text{Tr} \int \frac{d\mathbf{q}}{(2\pi)^3} \left(\Psi^+(\mathbf{q}) \Lambda_+^+(\mathbf{q}) \Psi(\mathbf{q}) \Lambda_-(\mathbf{q}) - \Psi^+(\mathbf{q}) \Lambda_+^-(\mathbf{q}) \Psi(\mathbf{q}) \Lambda_+(\mathbf{q}) \right) = 2M. \quad (\text{B6})$$

Note that due to the covariant formulation of the normalization condition, the wave function is correctly normalized in any frame.

By taking the trace in (B6) for the different states we find the following normalization conditions:

$$0^{-+} : \quad 2M = \frac{8}{m} \int_0^{\infty} \frac{dq}{(2\pi)^3} q^2 E(q) \Psi_A(q) \Psi_P(q), \quad (\text{B7})$$

$$1^{--} : \quad 2M = 8 \int_0^{\infty} \frac{dq}{(2\pi)^3} q^2 \left(\frac{E(q)}{q} \Psi_S(q) \Psi_{T_1}(q) + \frac{E(q)}{m} \Psi_{T_2}(q) \Psi_V(q) \right), \quad (\text{B8})$$

$$1^{+-} : \quad 2M = \frac{8}{m} \int_0^{\infty} \frac{dq}{(2\pi)^3} q^2 E(q) \Psi_A(q) \Psi_P(q), \quad (\text{B9})$$

$$0^{++} : \quad 2M = 8 \int_0^{\infty} \frac{dq}{(2\pi)^3} q E(q) \Psi_S(q) \Psi_T(q), \quad (\text{B10})$$

$$1^{++} : \quad 2M = -8 \int_0^{\infty} \frac{dq}{(2\pi)^3} q^2 \frac{E(q)}{m} \Psi_V(q) \Psi_T(q), \quad (\text{B11})$$

$$2^{++} : \quad 2M = 8 \int_0^{\infty} \frac{dq}{(2\pi)^3} q^2 \left(\frac{E(q)}{q} \Psi_S(q) \Psi_{T_1}(q) + \frac{E(q)}{m} \Psi_{T_2}(q) \Psi_V(q) \right). \quad (\text{B12})$$

APPENDIX C: EIGENVALUE EQUATIONS FOR THE DIFFERENT STATES

Equations for the scalar amplitudes of the different states can be found from (11). By expanding both sides of (11) in the Dirac algebra, and then multiplying by $(Y_{\ell m} \hat{\mathbf{q}})^*$ or $(\mathbf{Y}_{\ell m}^{(e)}(\hat{\mathbf{q}}))^*$ and summing over m , and finally integrating over the angular variables we get the equations below [1]. The functions $F_{\ell}^V(p, q)$ and $F_{\ell}^S(p, q)$ are the coefficients of the spherical harmonics in the expansion of the kernel given in Section III. The function $F_{\ell}^{Vc}(p, q)$ is the same as $F_{\ell}^V(p, q)$, but the terms with $F_{\ell}^{Vc}(p, q)$ only appear in the Coulomb gauge. Thus, in the Feynman gauge, these terms should be set to zero.

0^{-+} state

$$\begin{aligned}
M\Psi_P(q) &= \left(\frac{2E(q)^2}{m} + U \frac{m}{E(q)} \left(1 - \frac{q^2}{m^2} \right) \right) \Psi_A(q) \\
&\quad + \frac{m}{E(q)} \int_0^\infty \frac{dp}{(2\pi)^3} p^2 \left(F_0^S(p, q) - \frac{pq}{m^2} F_1^S(p, q) \right) \Psi_A(p) \\
&\quad + \frac{m}{E(q)} \int_0^\infty \frac{dp}{(2\pi)^3} p^2 \left(2F_0^V(p, q) - F_0^{Vc}(p, q) - \frac{pq}{m^2} F_1^{Vc}(p, q) \right) \Psi_A(p), \quad (C1)
\end{aligned}$$

$$\begin{aligned}
M\Psi_A(q) &= m \left(2 + \frac{U}{E(q)} \right) \Psi_P(q) \\
&\quad + \frac{m}{E(q)} \int_0^\infty \frac{dp}{(2\pi)^3} p^2 (F_0^S(p, q) - 4F_0^V(p, q) + F_0^{Vc}(p, q)) \Psi_P(p). \quad (C2)
\end{aligned}$$

1^{--} state

$$\begin{aligned}
M\Psi_{T_1}(q) &= \left(\frac{2E(q)^2}{q} + \frac{U}{qE(q)} (m^2 - q^2) \right) \Psi_S(q) \\
&\quad - \frac{1}{E(q)} \int_0^\infty \frac{dp}{(2\pi)^3} p^2 \left(\left(qF_1^S - \frac{m^2}{3p} (F_0^S + 2F_2^S) \right) \Psi_S(p) - m \frac{\sqrt{2}}{3} (F_0^S - F_2^S) \Psi_V(p) \right) \\
&\quad - \frac{1}{E(q)} \int_0^\infty \frac{dp}{(2\pi)^3} p^2 \left(\left(q(4F_1^V - F_1^{Vc}) + \frac{m^2}{3p} (2F_0^V + F_0^{Vc} + 4(F_2^V - F_2^{Vc})) \right) \Psi_S(p) \right. \\
&\quad \quad \left. + \left(m \frac{2\sqrt{2}}{3} (F_0^V - F_2^V) - \frac{m(p^2 - q^2)\sqrt{2}}{2pq} F_1^{Vc} \right) \Psi_V(p) \right), \quad (C3)
\end{aligned}$$

$$\begin{aligned}
M\Psi_{T_2}(q) &= m \left(2 + \frac{U}{E(q)} \right) \Psi_V(q) \\
&\quad + \frac{1}{E(q)} \int_0^\infty \frac{dp}{(2\pi)^3} p^2 \left(\frac{\sqrt{2}m^2}{3p} (F_0^S - F_2^S) \Psi_S(p) + \frac{m}{3} (2F_0^S + F_2^S) \Psi_V(p) \right) \\
&\quad - \frac{1}{E(q)} \int_0^\infty \frac{dp}{(2\pi)^3} p^2 \left(\frac{\sqrt{2}m^2}{p} \left(\frac{2}{3} (F_0^V - F_2^V) + \frac{(p^2 - q^2)}{2pq} F_1^{Vc} \right) \Psi_S(p) \right. \\
&\quad \quad \left. + \frac{2m}{3} (2F_0^V - F_0^{Vc} + F_2^V + F_2^{Vc}) \Psi_V(p) \right), \quad (C4)
\end{aligned}$$

$$\begin{aligned}
M\Psi_S(q) &= q \left(2 + \frac{U}{E(q)} \right) \Psi_{T_1}(q) \\
&\quad + \frac{1}{E(q)} \int_0^\infty \frac{dp}{(2\pi)^3} p^2 \left(\frac{q}{3} (F_0^S + 2F_2^S) \Psi_{T_1}(p) + \frac{\sqrt{2}q}{3} (F_0^S - F_2^S) \Psi_{T_2}(p) \right) \\
&\quad + \frac{1}{E(q)} \int_0^\infty \frac{dp}{(2\pi)^3} p^2 \left(\frac{p}{3} (F_0^{Vc} - 4F_2^{Vc}) \Psi_{T_1}(p) - \frac{(p^2 - q^2)\sqrt{2}}{2p} F_1^{Vc} \Psi_{T_2}(p) \right), \quad (C5)
\end{aligned}$$

$$M\Psi_V(q) = \left(\frac{2E(q)^2}{m} + U \frac{m}{E(q)} \left(1 - \frac{q^2}{m^2} \right) \right) \Psi_{T_2}(q)$$

$$\begin{aligned}
& + \frac{1}{E(q)} \int_0^\infty \frac{dp}{(2\pi)^3} p^2 \left(\frac{\sqrt{2}m}{3} (F_0^S - F_2^S) \Psi_{T_1}(p) + \left(\frac{m}{3} (2F_0^S + F_2^S) - \frac{pq}{m} F_1^S \right) \Psi_{T_2}(p) \right) \\
& + \frac{1}{E(q)} \int_0^\infty \frac{dp}{(2\pi)^3} p^2 \left(\frac{m(p^2 - q^2)\sqrt{2}}{2q^2} F_1^{Vc} \Psi_{T_1}(p) - \left(\frac{2pq}{m} F_1^V + \frac{2m}{3} (F_0^{Vc} - F_2^{Vc}) \right) \Psi_{T_2}(p) \right). \quad (C6)
\end{aligned}$$

1⁺⁻ state

$$\begin{aligned}
M\Psi_P(q) &= \left(\frac{2E(q)^2}{m} + U \frac{m}{E(q)} \left(1 - \frac{q^2}{m^2} \right) \right) \Psi_A(q) \\
&+ \frac{m}{E(q)} \int_0^\infty \frac{dp}{(2\pi)^3} p^2 \left(F_1^S - \frac{pq}{3m^2} (F_0^S + 2F_2^S) \right) \Psi_A(p) \\
&+ \frac{m}{E(q)} \int_0^\infty \frac{dp}{(2\pi)^3} p^2 \left(2F_1^V - F_1^{Vc} + \frac{pq}{3m^2} (F_0^{Vc} - 4F_2^{Vc}) \right) \Psi_A(p), \quad (C7)
\end{aligned}$$

$$\begin{aligned}
M\Psi_A(q) &= m \left(2 + \frac{U}{E(q)} \right) \Psi_P(q) \\
&+ \frac{m}{E(q)} \int_0^\infty \frac{dp}{(2\pi)^3} p^2 (F_1^S - 4F_1^V + F_1^{Vc}) \Psi_P(p). \quad (C8)
\end{aligned}$$

0⁺⁺ state

$$\begin{aligned}
M\Psi_T(q) &= \left(\frac{2E(q)^2}{q} + \frac{U}{qE(q)} (m^2 - q^2) \right) \Psi_S(q) \\
&- \frac{1}{E(q)} \int_0^\infty \frac{dp}{(2\pi)^3} p^2 \left(qF_0^S - \frac{m^2}{p} F_1^S \right) \Psi_S(p) \\
&- \frac{1}{E(q)} \int_0^\infty \frac{dp}{(2\pi)^3} p^2 \left(q(4F_0^V - F_0^{Vc}) + \frac{m^2}{p} (2F_1^V - F_1^{Vc}) \right) \Psi_S(p), \quad (C9)
\end{aligned}$$

$$\begin{aligned}
M\Psi_S(q) &= q \left(2 + \frac{U}{E(q)} \right) \Psi_T(q) \\
&+ \frac{1}{E(q)} \int_0^\infty \frac{dp}{(2\pi)^3} p^2 q (F_1^S - F_1^{Vc}) \Psi_T(p). \quad (C10)
\end{aligned}$$

1⁺⁺ state

$$\begin{aligned}
M\Psi_T(q) &= -m \left(2 + \frac{U}{E(q)} \right) \Psi_V(q) \\
&- \frac{m}{E(q)} \int_0^\infty \frac{dp}{(2\pi)^3} p^2 (F_1^S - 2F_1^V) \Psi_V(p), \quad (C11) \\
M\Psi_V(q) &= - \left(\frac{2E(q)^2}{m} + U \frac{m}{E(q)} \left(1 - \frac{q^2}{m^2} \right) \right) \Psi_T(q)
\end{aligned}$$

$$\begin{aligned}
& - \frac{m}{E(q)} \int_0^\infty \frac{dp}{(2\pi)^3} p^2 \left(F_1^S - \frac{pq}{3m^2} (2F_0^S + F_2^S) \right) \Psi_T(p) \\
& + \frac{2}{3E(q)m} \int_0^\infty \frac{dp}{(2\pi)^3} p^2 \left(pq(2F_0^V + F_2^V) - q^2(F_0^{Vc} - F_2^{Vc}) \right) \Psi_T(p). \tag{C12}
\end{aligned}$$

2⁺⁺ state

$$\begin{aligned}
M\Psi_{T_1}(q) &= \left(\frac{2E(q)^2}{q} + \frac{U}{qE(q)}(m^2 - q^2) \right) \Psi_S(q) \\
& - \frac{1}{E(q)} \int_0^\infty \frac{dp}{(2\pi)^3} p^2 \left(\left(qF_2^S - \frac{m^2}{5p} (2F_1^S + 3F_3^S) \right) \Psi_S(p) - m \frac{\sqrt{6}}{5} (F_1^S - F_3^S) \Psi_V(p) \right) \\
& - \frac{1}{E(q)} \int_0^\infty \frac{dp}{(2\pi)^3} p^2 \left(\left(q(4F_2^V - F_2^{Vc}) + \frac{m^2}{5p} (4(F_1^V + F_1^{Vc}) + 3(2F_3^V - 3F_3^{Vc})) \right) \Psi_S(p) \right. \\
& \left. + \left(m \frac{2\sqrt{6}}{5} (F_1^V - F_3^V) - m \frac{(p^2 - q^2)\sqrt{6}}{2pq} F_2^{Vc} \right) \Psi_V(p) \right), \tag{C13}
\end{aligned}$$

$$\begin{aligned}
M\Psi_{T_2}(q) &= m \left(2 + \frac{U}{E(q)} \right) \Psi_V(q) \\
& + \frac{1}{E(q)} \int_0^\infty \frac{dp}{(2\pi)^3} p^2 \left(\frac{\sqrt{6}m^2}{5p} (F_1^S - F_3^S) \Psi_S(p) + \frac{m}{5} (3F_1^S + 2F_3^S) \Psi_V(p) \right) \\
& - \frac{1}{E(q)} \int_0^\infty \frac{dp}{(2\pi)^3} p^2 \left(\left(\frac{2\sqrt{6}m^2}{5p} (F_1^V - F_3^V) + \frac{m^2(p^2 - q^2)\sqrt{6}}{2p^2q} F_2^{Vc} \right) \Psi_S(p) \right. \\
& \left. + \frac{2m}{5} (3(F_1^V - F_1^{Vc}) + (2F_3^V + 3F_3^{Vc})) \Psi_V(p) \right), \tag{C14}
\end{aligned}$$

$$\begin{aligned}
M\Psi_S(q) &= q \left(2 + \frac{U}{E(q)} \right) \Psi_{T_1}(q) \\
& + \frac{1}{E(q)} \int_0^\infty \frac{dp}{(2\pi)^3} p^2 \left(\frac{q}{5} (2F_1^S + 3F_3^S) \Psi_{T_1}(p) + \frac{\sqrt{6}q}{5} (F_1^S - F_3^S) \Psi_{T_2}(p) \right) \\
& + \frac{1}{E(q)} \int_0^\infty \frac{dp}{(2\pi)^3} p^2 \left(\frac{p}{5} (4F_1^{Vc} - 9F_3^{Vc}) \Psi_{T_1}(p) - \frac{(p^2 - q^2)\sqrt{6}}{2p} F_2^{Vc} \Psi_{T_2}(p) \right), \tag{C15}
\end{aligned}$$

$$\begin{aligned}
M\Psi_V(q) &= \left(\frac{2E(q)^2}{m} + U \frac{m}{E(q)} \left(1 - \frac{q^2}{m^2} \right) \right) \Psi_{T_2}(q) \\
& + \frac{1}{E(q)} \int_0^\infty \frac{dp}{(2\pi)^3} p^2 \left(\frac{\sqrt{6}m}{5} (F_1^S - F_3^S) \Psi_{T_1}(p) + \left(\frac{m}{5} (3F_1^S + 2F_3^S) - \frac{pq}{m} F_2^S \right) \Psi_{T_2}(p) \right) \\
& + \frac{1}{E(q)} \int_0^\infty \frac{dp}{(2\pi)^3} p^2 \left(\frac{(p^2 - q^2)\sqrt{6}}{2q^2} F_2^{Vc} \Psi_{T_1}(p) - \left(\frac{2pq}{m} F_2^V + \frac{6}{5} (F_1^{Vc} - F_3^{Vc}) \right) \Psi_{T_2}(p) \right). \tag{C16}
\end{aligned}$$

APPENDIX D: AMPLITUDES FOR THE DIFFERENT STATES

For calculation of different decay amplitudes we need the expressions for the wave functions $\chi(q)$ for the different states. Like the reduced wave function, $\Psi(\mathbf{q})$, $\chi(q)$ is expanded in the Dirac algebra by imposing the correct transformation properties regarding angular momentum, parity, and charge parity. The scalar amplitudes of this expansion are then expressed in the amplitudes of $\Psi(\mathbf{q})$, by similarly expanding (10) in the Dirac algebra using the wave functions given in Appendix A.

0^{-+} state

The most general wave function for the 0^{-+} state can be written

$$\chi(q) = (\chi_A(q)\gamma^5 + \chi_B(q)\gamma^5(\boldsymbol{\gamma} \cdot \mathbf{q}) + \chi_C(q)\gamma^5\gamma^0 + \chi_D(q)\gamma^5(\boldsymbol{\alpha} \cdot \mathbf{q}))Y_{00}(\hat{\mathbf{q}}). \quad (\text{D1})$$

The scalar amplitudes $\chi_i(q)$ are

$$\chi_A(q) = (\Delta^{+-} + \Delta^{-+})\frac{1}{2}\Psi_P(q) + (\Delta^{+-} - \Delta^{-+})\frac{E}{2m}\Psi_A(q), \quad (\text{D2})$$

$$\chi_B(q) = (\Delta^{--} - \Delta^{++})\frac{1}{E}I_0(q), \quad (\text{D3})$$

$$\begin{aligned} \chi_C(q) = & -(\Delta^{+-} + \Delta^{-+})\frac{1}{2}\Psi_A(q) - (\Delta^{+-} - \Delta^{-+})\frac{m}{2E}\Psi_P(q) \\ & + (\Delta^{--} + \Delta^{++})\frac{q^2}{E^2}I_0(q), \end{aligned} \quad (\text{D4})$$

$$\begin{aligned} \chi_D(q) = & (\Delta^{+-} + \Delta^{-+})\frac{1}{2m}\Psi_A(q) + (\Delta^{+-} - \Delta^{-+})\frac{1}{2E}\Psi_P(q) \\ & + (\Delta^{--} + \Delta^{++})\frac{m}{E^2}I_0(q), \end{aligned} \quad (\text{D5})$$

where

$$\Delta^{+-} = -\frac{i(M-2E)}{(M/2+q^0-E+i\epsilon)(-M/2+q^0+E-i\epsilon)}, \quad (\text{D6})$$

$$\Delta^{-+} = \frac{i(M+2E)}{(M/2+q^0+E-i\epsilon)(-M/2+q^0-E+i\epsilon)}, \quad (\text{D7})$$

$$\Delta^{++} = \frac{i}{(M/2+q^0-E+i\epsilon)(-M/2+q^0-E+i\epsilon)}, \quad (\text{D8})$$

$$\Delta^{--} = \frac{i}{(M/2+q^0+E-i\epsilon)(-M/2+q^0+E-i\epsilon)}. \quad (\text{D9})$$

The integral $I_0(q)$ is

$$\begin{aligned} I_0(q) = & U\Psi_A(q) + \frac{1}{2} \int \frac{dp}{(2\pi)^3} p^2 (F_0^S(p, q) + \frac{p}{q} F_1^S(p, q)) \Psi_A(p) \\ & + \int \frac{dp}{(2\pi)^3} p^2 \left(F_0^V(p, q) - \frac{1}{2} \left(F_0^{Vc} - \frac{p}{q} F_1^{Vc} \right) \right) \Psi_A(p). \end{aligned} \quad (\text{D10})$$

1^{- -} state

The wave function for the 1^{- -} state can be expanded as

$$\begin{aligned} \chi(q) = & (\chi_1(q) + \chi_2(q)\gamma^0 + \chi_3(q)(\boldsymbol{\gamma} \cdot \mathbf{q}) + \chi_4(q)(\boldsymbol{\alpha} \cdot \mathbf{q}))Y_{1m}(\hat{\mathbf{q}}) \\ & + (\chi_5(q)\boldsymbol{\gamma} + \chi_6(q)\boldsymbol{\alpha} + i\chi_7(q)\gamma^5(\boldsymbol{\alpha} \times \mathbf{q}) + i\chi_8(q)\gamma^5(\mathbf{q} \times \boldsymbol{\gamma})) \cdot \mathbf{Y}_{1m}^{(e)}(\hat{\mathbf{q}}). \end{aligned} \quad (\text{D11})$$

The amplitudes are

$$\begin{aligned} \chi_1(q) = & (\Delta^{+-} + \Delta^{-+})\frac{1}{2}\Psi_S(q) + (\Delta^{+-} - \Delta^{-+})\frac{q}{2E}\Psi_{T_1}(q) \\ & + (\Delta^{++} + \Delta^{--})\frac{m}{E^2}I_1(q), \end{aligned} \quad (\text{D12})$$

$$\chi_2(q) = (\Delta^{++} - \Delta^{--})\frac{1}{E}I_1(q), \quad (\text{D13})$$

$$\begin{aligned} \chi_3(q) = & (\Delta^{+-} + \Delta^{-+})\frac{m}{2q^2}\Psi_S(q) + (\Delta^{+-} - \Delta^{-+})\frac{m}{2Eq}\Psi_{T_1}(q) \\ & - (\Delta^{++} + \Delta^{--})\frac{1}{E^2}I_1(q), \end{aligned} \quad (\text{D14})$$

$$\chi_4(q) = (\Delta^{+-} + \Delta^{-+})\frac{1}{2q}\Psi_{T_1}(q) + (\Delta^{+-} - \Delta^{-+})\frac{E}{2q^2}\Psi_S(q), \quad (\text{D15})$$

$$\chi_5(q) = (\Delta^{+-} + \Delta^{-+})\frac{1}{2}\Psi_V(q) + (\Delta^{+-} - \Delta^{-+})\frac{E}{2m}\Psi_{T_2}(q), \quad (\text{D16})$$

$$\begin{aligned} \chi_6(q) = & (\Delta^{+-} + \Delta^{-+})\frac{1}{2}\Psi_{T_2}(q) + (\Delta^{+-} - \Delta^{-+})\frac{m}{2E}\Psi_V(q) \\ & + (\Delta^{++} + \Delta^{--})\frac{q^2}{E^2}I_2(q), \end{aligned} \quad (\text{D17})$$

$$\chi_7(q) = (\Delta^{++} - \Delta^{--})\frac{1}{E}I_2(q), \quad (\text{D18})$$

$$\begin{aligned} \chi_8(q) = & -(\Delta^{+-} + \Delta^{-+})\frac{1}{2m}\Psi_{T_2}(q) - (\Delta^{+-} - \Delta^{-+})\frac{1}{2E}\Psi_V(q) \\ & + (\Delta^{++} + \Delta^{--})\frac{m}{E^2}I_2(q), \end{aligned} \quad (\text{D19})$$

where

$$\begin{aligned} I_1(q) = & mU\Psi_S(q) \\ & + \frac{1}{2} \int \frac{dp}{(2\pi)^3} p^2 \left(\left(mF_1^S + \frac{mq}{3p}(F_0^S + 2F_2^S) \right) \Psi_S(p) + q\frac{\sqrt{2}}{3}(F_0^S - F_2^S)\Psi_V(p) \right) \\ & + \int \frac{dp}{(2\pi)^3} p^2 \left(\left(2mF_1^V - \frac{mq}{3p}(F_0^V + 2F_2^V) + m\frac{q}{2p} \left(\frac{q}{p}F_1^{Vc} - F_0^{Vc} \right) \right) \Psi_S(p) \right. \\ & \left. - \left(q\frac{\sqrt{2}}{3}(F_0^V - F_2^V) - \frac{(p^2 - q^2)}{2\sqrt{2}p}F_1^{Vc} \right) \Psi_V(p) \right), \end{aligned} \quad (\text{D20})$$

$$\begin{aligned} I_2(q) = & -U\Psi_{T_2}(q) \\ & - \frac{1}{2} \int \frac{dp}{(2\pi)^3} p^2 \left(\frac{\sqrt{2}}{3}(F_0^S - F_2^S)\Psi_{T_1}(p) + \left(\frac{p}{q}F_1^S + \frac{1}{3}(2F_0^S + F_2^S) \right) \Psi_{T_2}(p) \right) \end{aligned}$$

$$- \int \frac{dp}{(2\pi)^3} p^2 \left(\frac{(p^2 - q^2)}{2\sqrt{2}pq} F_1^{Vc} \Psi_{T_1}(p) + \left(\frac{p}{q} F_1^V - \frac{1}{3} (F_0^{Vc} - F_2^{Vc}) \right) \Psi_{T_2}(p) \right). \quad (\text{D21})$$

0⁺⁺ state

The wave function for the 0⁺⁺ state can be expanded as

$$\chi(q) = (\chi_1(q) + \chi_2(q)\gamma^0 + \chi_3(q)(\boldsymbol{\gamma} \cdot \mathbf{q}) + \chi_4(q)(\boldsymbol{\alpha} \cdot \mathbf{q})) Y_{00}(\hat{\mathbf{q}}). \quad (\text{D22})$$

The amplitudes are the same as for 1⁻⁻ but with $I_1(q)$ given by

$$\begin{aligned} I_1(q) &= mU\Psi_S(q) + \frac{1}{2} \int \frac{dp}{(2\pi)^3} p^2 \left(mF_0^S + \frac{mq}{p} F_1^S \right) \Psi_S(p) \\ &+ \int \frac{dp}{(2\pi)^3} p^2 \left(2mF_0^V - \frac{mq}{p} F_1^V + \frac{m}{2} \left(\frac{q}{p} F_1^{Vc} - F_0^{Vc} \right) \right) \Psi_S(p). \end{aligned} \quad (\text{D23})$$

1⁺⁺ state

The wave function for the 1⁺⁺ state can be expanded as

$$\begin{aligned} \chi(q) &= (\chi_1(q)\gamma^5 + \chi_2(q)\gamma^5\gamma^0 + \chi_3(q)\gamma^5(\boldsymbol{\gamma} \cdot \mathbf{q}) + \chi_4(q)\gamma^5(\boldsymbol{\alpha} \cdot \mathbf{q})) Y_{1m}(\hat{\mathbf{q}}) \\ &+ (\chi_5(q)\gamma^5\boldsymbol{\gamma} + \chi_6(q)\gamma^5\boldsymbol{\alpha} + i\chi_7(q)(\boldsymbol{\alpha} \times \mathbf{q}) + i\chi_8(q)(\mathbf{q} \times \boldsymbol{\gamma})) \cdot \mathbf{Y}_{1m}^{(e)}(\hat{\mathbf{q}}). \end{aligned} \quad (\text{D24})$$

The amplitudes are

$$\chi_1(q) = 0, \quad (\text{D25})$$

$$\chi_2(q) = (\Delta^{--} - \Delta^{++}) \frac{q}{Em} I_1(q), \quad (\text{D26})$$

$$\chi_3(q) = (\Delta^{++} + \Delta^{--}) \frac{1}{mq} I_1(q), \quad (\text{D27})$$

$$\chi_4(q) = (\Delta^{--} - \Delta^{++}) \frac{1}{Eq} I_1(q), \quad (\text{D28})$$

$$\begin{aligned} \chi_5(q) &= -(\Delta^{+-} - \Delta^{-+}) \frac{q}{2E} \Psi_V(q) + (\Delta^{+-} + \Delta^{-+}) \frac{q}{2m} \Psi_T(q) \\ &+ (\Delta^{++} + \Delta^{--}) \frac{m}{E^2} I_2(q), \end{aligned} \quad (\text{D29})$$

$$\chi_6(q) = (\Delta^{--} - \Delta^{++}) \frac{1}{E} I_2(q), \quad (\text{D30})$$

$$\begin{aligned} \chi_7(q) &= -(\Delta^{+-} - \Delta^{-+}) \frac{m}{2Eq} \Psi_V(q) + (\Delta^{+-} + \Delta^{-+}) \frac{1}{2q} \Psi_T(q) \\ &- (\Delta^{++} + \Delta^{--}) \frac{1}{E^2} I_2(q), \end{aligned} \quad (\text{D31})$$

$$\chi_8(q) = (\Delta^{+-} - \Delta^{-+}) \frac{1}{2q} \Psi_V(q) - (\Delta^{+-} + \Delta^{-+}) \frac{E}{2qm} \Psi_T(q), \quad (\text{D32})$$

where

$$I_1(q) = \frac{1}{2} \int \frac{dp}{(2\pi)^3} p^3 \frac{\sqrt{2}}{3} (F_0^S - F_2^S) \Psi_T(p) - \int \frac{dp}{(2\pi)^3} p^2 \left(p \frac{\sqrt{2}}{3} (F_0^V - F_2^V) + \frac{(p^2 - q^2)}{2\sqrt{2}q} F_1^{Vc} \right) \Psi_T(p), \quad (\text{D33})$$

$$I_2(q) = qU \Psi_T(q) + \frac{1}{2} \int \frac{dp}{(2\pi)^3} p^2 \left(qF_1^S + \frac{p}{3} (2F_0^S + F_2^S) \right) \Psi_T(p) - \int \frac{dp}{(2\pi)^3} p^2 \left(\frac{p}{3} (2F_0^V + F_2^V) - \frac{p^2}{4q} \left((p^2 + q^2) F_1^{Vc} - 2pq F_0^{Vc} \right) \right) \Psi_T(p). \quad (\text{D34})$$

2⁺⁺ state

The expansion for the 2⁺⁺ state is the same as for the 1⁻⁻ state with the changes $Y_{1m} \rightarrow Y_{2m}$, $\mathbf{Y}_{1m}^{(e)} \rightarrow \mathbf{Y}_{2m}^{(e)}$. The amplitudes are the same but with $I_1(q)$ and $I_2(q)$ given by

$$I_1(q) = mU \Psi_S(q) + \frac{1}{2} \int \frac{dp}{(2\pi)^3} p^2 \left(\left(mF_2^S + \frac{mq}{5p} (2F_1^S + 3F_3^S) \right) \Psi_S(p) + q \frac{\sqrt{6}}{5} (F_1^S - F_3^S) \Psi_V(p) \right) + \int \frac{dp}{(2\pi)^3} p^2 \left(\left(2mF_2^V - \frac{mq}{5p} (2F_1^V + 3F_3^V) + \frac{m}{4p^2} \left((p^2 + 3q^2) F_2^{Vc} - 4pq F_1^{Vc} \right) \right) \Psi_S(p) - \left(q \frac{\sqrt{6}}{5} (F_1^V - F_3^V) - \frac{(p^2 - q^2) \sqrt{6}}{4p} F_2^{Vc} \right) \Psi_V(p) \right), \quad (\text{D35})$$

$$I_2(q) = -U \Psi_{T_2}(q) - \frac{1}{2} \int \frac{dp}{(2\pi)^3} p^2 \left(\frac{\sqrt{6}}{5} (F_1^S - F_3^S) \Psi_{T_1}(p) + \left(\frac{p}{q} F_2^S + \frac{1}{5} (3F_1^S + 2F_3^S) \right) \Psi_{T_2}(p) \right) - \int \frac{dp}{(2\pi)^3} p^2 \left(\frac{(p^2 - q^2) \sqrt{6}}{4pq} F_2^{Vc} \Psi_{T_1}(p) + \left(\frac{p}{q} F_2^V + \frac{1}{2pq} \left((p^2 + q^2) F_2^{Vc} - 2pq F_1^{Vc} \right) \right) \Psi_{T_2}(p) \right). \quad (\text{D36})$$

1. Lorentz transformed states

To calculate the E1 and M1 transitions we need the wave functions for some states in a frame where the particle is moving with momentum P .

The Salpeter equation in a general frame (1) is found from the one in the rest frame as follows. First this is multiplied by the spinor transformation matrices $S(\Lambda)$ and $S^{-1}(\Lambda)$ on each side. Λ is the Lorentz matrix transforming $(M, \mathbf{0})$ to the momentum P . Then the change of variables $q \rightarrow \Lambda^{-1}q$ is made.

The Lorentz transformed state is therefore found to be

$$\chi(q, P) = S(\Lambda)\chi(\Lambda^{-1}q, M)S^{-1}(\Lambda), \quad (\text{D37})$$

where $\chi(q, M)$ is the wave function in the rest frame. Under the change of variables $q \rightarrow \Lambda^{-1}q$, then

$$q^0 \rightarrow q_P = \frac{q \cdot P}{M}, \quad (\text{D38})$$

$$|\mathbf{q}| \rightarrow q_\top = \sqrt{-q_\perp^2}, \quad q_\perp = q - \frac{q \cdot P}{M^2}P, \quad (\text{D39})$$

$$E \rightarrow \omega = \sqrt{q_\top^2 + m^2}, \quad (\text{D40})$$

$$\sin \theta \rightarrow \sin \theta' = \frac{\sqrt{q_x^2 + q_y^2}}{q_\top}, \quad (\text{D41})$$

$$\cos \theta \rightarrow \cos \theta' = \frac{-q^0 P_z + q_z P^0}{M q_\top}, \quad (\text{D42})$$

if the particle moves in the z direction.

For the 0^{-+} state the transformed wave function is

$$\chi(q, P) = \left(\chi_A(q)\gamma^5 - \chi_B(q)\gamma^5 \not{q}_\perp + \chi_C(q)\gamma^5 \frac{P}{M} + \chi_D(q)\frac{\gamma^5}{2M}(\not{q}_\perp P - P \not{q}_\perp) \right) Y_{00}(\theta', \varphi). \quad (\text{D43})$$

The scalar amplitudes are the same as before with the above changes of variables, and with the functions Ψ_i depending on q_\top .

The Lorentz transformed 1^{--} wave function is

$$\begin{aligned} \chi(q, P) = & \left(\chi_1 + \chi_2 \frac{P}{M} - \chi_3 \not{q}_\perp + \chi_4 \frac{1}{2M}(\not{q}_\perp P - P \not{q}_\perp) \right) Y_{1m}(\theta', \varphi) \\ & - \chi_5 \not{Y} + \frac{\chi_6}{2M}(\not{Y} P - P \not{Y}) + \frac{\chi_7}{2}(\not{Y} \not{q}_\perp - \not{q}_\perp \not{Y}) + \chi_8 \frac{P}{2M}(\not{Y} \not{q}_\perp - \not{q}_\perp \not{Y}). \end{aligned} \quad (\text{D44})$$

Here

$$Y = \left(\frac{P_z}{M} Y_z, Y_x, Y_y, \frac{P^0}{M} Y_z \right) \quad (\text{D45})$$

with

$$\mathbf{Y} = (Y_x(\theta', \varphi), Y_y(\theta', \varphi), Y_z(\theta', \varphi)). \quad (\text{D46})$$

The Lorentz transformed wave functions for 0^{++} and 2^{++} are identical to the one for 1^{--} (only the first four terms for 0^{++}).

The wave function for 1^{++} is

$$\begin{aligned} \chi = & \left(\chi_1 \gamma^5 + \chi_2 \gamma^5 \frac{P}{M} - \chi_3 \gamma^5 \not{q}_\perp + \chi_4 \frac{\gamma^5}{2M}(\not{q}_\perp P - P \not{q}_\perp) \right) Y_{1m}(\theta', \varphi) \\ & - \chi_5 \gamma^5 \not{Y} + \chi_6 \frac{\gamma^5}{2M}(\not{Y} P - P \not{Y}) + \chi_7 \frac{\gamma^5}{2}(\not{Y} \not{q}_\perp - \not{q}_\perp \not{Y}) + \chi_8 \frac{\gamma^5}{2M} P(\not{Y} \not{q}_\perp - \not{q}_\perp \not{Y}). \end{aligned} \quad (\text{D47})$$

APPENDIX E: $\gamma\gamma$ DECAYS

We here present the matrix element for the $\gamma\gamma$ decays expressed in the scalar amplitudes defined in Appendix D. We write each scalar amplitude of the wave function as

$$\chi_i(q) = \chi_i^{+-}(q)\Delta^{+-} + \chi_i^{-+}(q)\Delta^{-+} + \chi_i^{++}(q)\Delta^{++} + \chi_i^{--}(q)\Delta^{--}, \quad (\text{E1})$$

where the Δ^{ij} 's are defined in (D6)-(D9). For example in (D2) we write

$$\chi_A(q) = \chi_A^{+-}(q)\Delta^{+-} + \chi_A^{-+}(q)\Delta^{-+} + \chi_A^{++}(q)\Delta^{++} + \chi_A^{--}(q)\Delta^{--}, \quad (\text{E2})$$

with

$$\chi_A^{+-} = \frac{1}{2}\Psi_P(q) + \frac{E}{2m}\Psi_A(q), \quad (\text{E3})$$

$$\chi_A^{-+} = \frac{1}{2}\Psi_P(q) - \frac{E}{2m}\Psi_A(q), \quad (\text{E4})$$

$$\chi_A^{++} = \chi_A^{--} = 0. \quad (\text{E5})$$

We then take the trace and perform the q^0 integration. This gives the following results.

0^{-+} state

$$\begin{aligned} \epsilon_1^\mu \epsilon_2^\nu M_{\mu\nu} = & -16i \int \frac{d\mathbf{q}}{(2\pi)^3} \frac{(\chi_C^{+-}(\mathbf{q}-\mathbf{k}) + \chi_D^{+-}m\mathbf{q}) \cdot (\boldsymbol{\epsilon}_1 \times \boldsymbol{\epsilon}_2)}{(M - 2E(\mathbf{q}) - 2E(\mathbf{q}-\mathbf{k}))E(\mathbf{q}-\mathbf{k})} \\ & + 16i \int \frac{d\mathbf{q}}{(2\pi)^3} \frac{(\chi_C^{-+}(\mathbf{q}-\mathbf{k}) + \chi_D^{-+}m\mathbf{q}) \cdot (\boldsymbol{\epsilon}_1 \times \boldsymbol{\epsilon}_2)}{(M + 2E(\mathbf{q}) + 2E(\mathbf{q}-\mathbf{k}))E(\mathbf{q}-\mathbf{k})} \\ & + 16i \int \frac{d\mathbf{q}}{(2\pi)^3} \frac{1}{(M - 2E(\mathbf{q}) - 2E(\mathbf{q}-\mathbf{k}))(M + 2E(\mathbf{q}) + 2E(\mathbf{q}-\mathbf{k}))E(\mathbf{q}-\mathbf{k})} \\ & \times \left[((\chi_B^{--} - \chi_B^{++})E(\mathbf{q}-\mathbf{k})\mathbf{q} \right. \\ & \left. + (\chi_C^{++} + \chi_C^{--})(\mathbf{q}-\mathbf{k}) + (\chi_D^{++} + \chi_D^{--})m\mathbf{q}) \cdot (\boldsymbol{\epsilon}_1 \times \boldsymbol{\epsilon}_2) \right]. \end{aligned} \quad (\text{E6})$$

0^{++} state

$$\begin{aligned} \epsilon_1^\mu \epsilon_2^\nu M_{\mu\nu} = & 16 \int \frac{d\mathbf{q}}{(2\pi)^3} \frac{(-m\chi_A^{+-} + \mathbf{q} \cdot (\mathbf{q}-\mathbf{k})\chi_C^{+-})(\boldsymbol{\epsilon}_1 \cdot \boldsymbol{\epsilon}_2) - 2\chi_C^{+-}(\boldsymbol{\epsilon}_1 \cdot \mathbf{q})(\boldsymbol{\epsilon}_2 \cdot \mathbf{q})}{(M - 2E(\mathbf{q}) - 2E(\mathbf{q}-\mathbf{k}))E(\mathbf{q}-\mathbf{k})} \\ & - 16 \int \frac{d\mathbf{q}}{(2\pi)^3} \frac{(-m\chi_A^{-+} + \mathbf{q} \cdot (\mathbf{q}-\mathbf{k})\chi_C^{-+})(\boldsymbol{\epsilon}_1 \cdot \boldsymbol{\epsilon}_2) - 2\chi_C^{-+}(\boldsymbol{\epsilon}_1 \cdot \mathbf{q})(\boldsymbol{\epsilon}_2 \cdot \mathbf{q})}{(M + 2E(\mathbf{q}) + 2E(\mathbf{q}-\mathbf{k}))E(\mathbf{q}-\mathbf{k})} \\ & - 16 \int \frac{d\mathbf{q}}{(2\pi)^3} \frac{1}{(M - 2E(\mathbf{q}) - 2E(\mathbf{q}-\mathbf{k}))(M + 2E(\mathbf{q}) + 2E(\mathbf{q}-\mathbf{k}))E(\mathbf{q}-\mathbf{k})} \\ & \times \left[(-m(\chi_A^{++} + \chi_A^{--}) + E(\mathbf{q}-\mathbf{k})(\chi_B^{--} - \chi_B^{++}) \right. \\ & \left. + \mathbf{q} \cdot (\mathbf{q}-\mathbf{k})(\chi_C^{++} + \chi_C^{--}))(\boldsymbol{\epsilon}_1 \cdot \boldsymbol{\epsilon}_2) - 2(\chi_C^{++} + \chi_C^{--})(\boldsymbol{\epsilon}_1 \cdot \mathbf{q})(\boldsymbol{\epsilon}_2 \cdot \mathbf{q}) \right]. \end{aligned} \quad (\text{E7})$$

2⁺⁺ state

$$\begin{aligned}
\epsilon_1^\mu \epsilon_2^\nu M_{\mu\nu} = & 16 \int \frac{d\mathbf{q}}{(2\pi)^3} \frac{1}{(M - 2E(\mathbf{q}) - 2E(\mathbf{q} - \mathbf{k}))E(\mathbf{q} - \mathbf{k})} \\
& \times \left[(-m\chi_1^{+-} + \mathbf{q} \cdot (\mathbf{q} - \mathbf{k})\chi_3^{+-})(\epsilon_1 \cdot \epsilon_2) - 2\chi_3^{+-}(\epsilon_1 \cdot \mathbf{q})(\epsilon_2 \cdot \mathbf{q}) \right. \\
& \left. + \chi_5^{+-} \cdot (\mathbf{q} - \mathbf{k})(\epsilon_1 \cdot \epsilon_2) - (\epsilon_1 \cdot \chi_5^{+-})(\epsilon_2 \cdot \mathbf{q}) - (\epsilon_1 \cdot \mathbf{q})(\epsilon_2 \cdot \chi_5^{+-}) \right] \\
& - 16 \int \frac{d\mathbf{q}}{(2\pi)^3} \frac{1}{(M + 2E(\mathbf{q}) + 2E(\mathbf{q} - \mathbf{k}))E(\mathbf{q} - \mathbf{k})} \\
& \times \left[(-m\chi_1^{-+} + \mathbf{q} \cdot (\mathbf{q} - \mathbf{k})\chi_3^{-+})(\epsilon_1 \cdot \epsilon_2) - 2\chi_3^{-+}(\epsilon_1 \cdot \mathbf{q})(\epsilon_2 \cdot \mathbf{q}) \right. \\
& \left. + \chi_5^{-+} \cdot (\mathbf{q} - \mathbf{k})(\epsilon_1 \cdot \epsilon_2) - (\epsilon_1 \cdot \chi_5^{-+})(\epsilon_2 \cdot \mathbf{q}) - (\epsilon_1 \cdot \mathbf{q})(\epsilon_2 \cdot \chi_5^{-+}) \right] \\
& - 16 \int \frac{d\mathbf{q}}{(2\pi)^3} \frac{1}{(M - 2E(\mathbf{q}) - 2E(\mathbf{q} - \mathbf{k}))(M + 2E(\mathbf{q}) + 2E(\mathbf{q} - \mathbf{k}))E(\mathbf{q} - \mathbf{k})} \\
& \times \left[(-m(\chi_1^{++} + \chi_1^{--}) + E(\mathbf{q} - \mathbf{k})(\chi_2^{--} - \chi_2^{++}) \right. \\
& + \mathbf{q} \cdot (\mathbf{q} - \mathbf{k})(\chi_3^{++} + \chi_3^{--}))(\epsilon_1 \cdot \epsilon_2) - 2(\chi_3^{++} + \chi_3^{--})(\epsilon_1 \cdot \mathbf{q})(\epsilon_2 \cdot \mathbf{q}) \\
& + (\chi_5^{++} + \chi_5^{--}) \cdot (\mathbf{q} - \mathbf{k})(\epsilon_1 \cdot \epsilon_2) - ((\epsilon_1 \cdot (\chi_5^{++} + \chi_5^{--}))(\epsilon_2 \cdot \mathbf{q}) \\
& \left. + (\epsilon_2 \cdot (\chi_5^{++} + \chi_5^{--}))(\epsilon_1 \cdot \mathbf{q})) \right]. \tag{E8}
\end{aligned}$$

Here $\chi_5(q) = \chi_5(q)\mathbf{Y}_{2m}^{(e)}(\hat{\mathbf{q}})$.

REFERENCES

- [1] L.G. Suttorp, *Ann. Phys.* 122 (1979) 397.
- [2] H.J. Munczek and P. Jain, *Phys. Rev. D* 46 (1992) 438; P. Jain and H.J. Munczek, *ibid.* 48 (1993) 5403.
- [3] J. Resag, C.R. Münz, B.C. Metsch, and H.R. Petry, *Nucl. Phys. A* 578 (1994) 397.
- [4] C.R. Münz, J. Resag, B.C. Metsch, and H.R. Petry, *Nucl. Phys. A* 578 (1994) 418.
- [5] J. Resag and C.R. Münz, *Nucl. Phys. A* 590 (1995) 735.
- [6] C.R. Münz, J. Resag, B.C. Metsch, and H.R. Petry, *Phys. Rev. C* 52 (1995) 2110.
- [7] T. Kugo, M.G. Mitchard, and Y. Yoshida, *Prog. Theor. Phys.* 91 (1994) 521.
- [8] M. Harada and Y. Yoshida, *Phys. Rev. D* 50 (1994) 6902.
- [9] M. Harada and Y. Yoshida, *Phys. Rev. D* 53 (1996) 1482.
- [10] M.G. Olsson, S. Veseli, and K. Williams, *Phys. Rev. D* 52 (1995) 5141.
- [11] J. Parramore and J. Piekarewicz, *Nucl. Phys. A* 585 (1995) 705.
- [12] J. Parramore, H.-C. Jean, and J. Piekarewicz, *Phys. Rev. C* 53 (1996) 2449.
- [13] M.G. Olsson, S. Veseli, and K. Williams, *Phys. Rev. D* 53 (1996) 504.
- [14] T. Murota, *Prog. Theor. Phys.* 69 (1983) 181.
- [15] H. Ito, *Prog. Theor. Phys.* 70 (1983) 499, *ibid.* 74 (1985) 1092.
- [16] J.-F. Lagaë, *Phys. Rev. D* 45 (1992) 305.
- [17] S. Mandelstam, *Proc. R. Soc. London Ser. A* 233 (1955) 248.
- [18] C.-H. Chang and Y.-Q. Chen, preprint AS-ITP-93-80, hep-ph/9401225.
- [19] H. Hershbach, *Phys. Rev. D* 47 (1993) 3027.
- [20] H. Ito, *Prog. Theor. Phys.* 67 (1982) 1553.
- [21] See e.g. G.L. Payne, in *Models and Methods in Few-Body Physics*, Proceedings of the Eighth Autumn School, Lisboa, Portugal, 1986, edited by L.S. Ferreira, A.C. Fonseca, and L. Streit, *Lecture Notes in Physics Vol. 273* (Springer, Berlin, 1987).
- [22] G. Hulth and H. Snellman, *Phys. Rev. D* 24 (1981) 2978.
- [23] D. Lurié, A.J. MacFarlane, Y. Takahashi, *Phys. Rev.* 140 (1965) B1091.
- [24] Particle Data Group, R.M. Barrett *et al.*, *Phys. Rev. D* 54 (1996) 1.
- [25] Cleo Collaboration, V. Savinov and R. Fulton, preprint hep-ex/9507006.

FIGURES

FIG. 1. Feynman diagram for lepton pair decays.

FIG. 2. Feynman diagrams for two gamma decays.

FIG. 3. Feynman diagrams for electromagnetic transitions.

FIG. 4. Amplitudes for the 0^{-+} state. We see that the function $\frac{m}{E}\Psi_P - \Psi_A$ appearing the negative energy part of the amplitude is much smaller than the function $\frac{m}{E}\Psi_P + \Psi_A$ in the positive energy part of the amplitude. However, the function I_0/E appearing in the mixed energy part is somewhere in between and certainly not negligible compared to the positive energy amplitude.

TABLES

TABLE I. Masses of the charmonium particles. The four columns in the middle contain the values obtained in the four different fits. F stands for Feynman gauge and C for Coulomb gauge, 10 MeV and 50 MeV stands for the minimum value of the experimental error, σ_i used in the fit. We see that all four fits give excellent agreement with experiments. In the last row we give χ^2 including all masses using an fictitious error of 10 MeV for all masses in order to make the numbers comparable. We see that the Coulomb gauge gives a slightly better result. Experimental values are taken from Review of Particle Properties data table [24].

particle	F 10 MeV	F 50 MeV	C 10 MeV	C 50 MeV	exp
$\eta_c(1S)$	2.97	2.97	2.97	2.97	2.98
$\eta_c(2S)$ [not used in fit]	3.62	3.64	3.62	3.63	3.59
J/Ψ	3.14	3.15	3.13	3.14	3.10
$\Psi(2S)$	3.70	3.72	3.69	3.70	3.69
$\Psi(2D)$	3.76	3.77	3.76	3.77	3.77
$\Psi(3S)$	4.09	4.10	4.09	4.10	4.04
$\Psi(3D)$	4.13	4.13	4.14	4.14	4.16
$\Psi(4S)$	4.39	4.39	4.40	4.39	4.42
χ_{c0}	3.44	3.41	3.43	3.41	3.42
χ_{c1}	3.50	3.51	3.50	3.52	3.51
χ_{c2}	3.49	3.50	3.49	3.51	3.56
h_{c1} [not used in fit]	3.49	3.50	3.49	3.51	3.53
χ^2	127	153	112	116	

TABLE II. Predicted values for the decay widths compared to the experimental values. The width $J/\Psi \rightarrow e^+e^-$ is used as input for the renormalization. The row with χ^2 values above the lepton decays presents the total χ^2 for the two gamma, E1, and M1 transitions, except $\Psi(2S) \rightarrow \eta_c\gamma$ which would otherwise totally dominate χ^2 . The last row is the total χ^2 for the lepton decay, but with the decays of the D states excluded, as they depend on higher order corrections not included in our calculations. Experimental values are taken from Review of Particle Properties data table [24] unless otherwise stated.

decay	F 10 MeV	F 50 MeV	C 10 MeV	C 50 MeV	exp
$\eta_c \rightarrow \gamma\gamma$	6.2	6.3	6.2	6.5	7.5 ± 1.5
$\chi_{c0} \rightarrow \gamma\gamma$	1.6	1.8	1.5	1.6	1.7 ± 1.3^a
$\chi_{c2} \rightarrow \gamma\gamma$	0.31	0.41	0.31	0.37	0.37 ± 0.17
$J/\Psi \rightarrow \eta_c\gamma$	1.65	1.33	1.66	1.38	1.14 ± 0.39
$\Psi(2S) \rightarrow \eta_c\gamma$	9.8	10.9	10.2	12.8	0.78 ± 0.24
$\Psi(2S) \rightarrow \eta'_c\gamma$	0.27	0.17	0.26	0.18	-
$\chi_{c0} \rightarrow J/\Psi\gamma$	130	96	143	110	92 ± 40
$\chi_{c1} \rightarrow J/\Psi\gamma$	390	399	426	434	240 ± 40
$\chi_{c2} \rightarrow J/\Psi\gamma$	218	195	240	218	267 ± 33
$\Psi(2S) \rightarrow \chi_{c0}\gamma$	31	47	26	31	26 ± 4
$\Psi(2S) \rightarrow \chi_{c1}\gamma$	58	49	63	50	24 ± 4
$\Psi(2S) \rightarrow \chi_{c2}\gamma$	48	47	51	49	22 ± 4
χ^2	136	127	174	116	
$J/\Psi \rightarrow e^+e^-$	5.26	5.26	5.26	5.26	5.26 ± 0.37
$\Psi(2S) \rightarrow e^+e^-$	2.81	2.45	2.92	2.68	2.14 ± 0.21
$\Psi(2D) \rightarrow e^+e^-$	0.09	0.19	0.25	0.35	0.26 ± 0.04
$\Psi(3S) \rightarrow e^+e^-$	1.99	1.59	2.09	1.84	0.75 ± 0.15
$\Psi(3D) \rightarrow e^+e^-$	0.14	0.29	0.05	0.07	0.77 ± 0.23
$\Psi(4S) \rightarrow e^+e^-$	1.42	1.00	1.56	1.31	0.47 ± 0.10
χ^2	169	62	212	130	

^aFrom Ref. [25]

TABLE III. Parameter values in the four fits and the value of χ^2 as defined in Eq. (38). When changing σ_i from 10 MeV to 50 MeV the parameters which change most are the quark mass m and the constant U . The parameter $\bar{\alpha}_s$ naturally changes significantly between the fits in the two different gauges, while the other parameters remain almost constant. We see that χ^2 is slightly smaller in the Coulomb gauge when $\sigma_i = 10$ MeV and slightly smaller in the Feynman gauge when $\sigma_i = 50$ MeV.

Parameter	F 10 MeV $\chi^2 = 110$	F 50 MeV $\chi^2 = 10.2$	C 10 MeV $\chi^2 = 95$	C 50 MeV $\chi^2 = 11.3$
$\bar{\alpha}_s$	0.282	0.288	0.348	0.369
m	1.366	1.276	1.358	1.298
λ	0.257	0.280	0.266	0.274
U	-0.131	0.072	-0.112	0.070

TABLE IV. Change of decay amplitudes when only the term with positive energy states is used. We see that most decay widths would increase, some with several 100%, when only the term with positive energy states is used. This shows that it is important to keep all terms in the model.

Decay	F 10 MeV	F 50 MeV	C 10 MeV	C 50 MeV
$J/\Psi \rightarrow \eta_c \gamma$	38%	66%	40%	60%
$\Psi(2S) \rightarrow \eta_c \gamma$	-47%	-67%	-59%	-68%
$\Psi(2S) \rightarrow \eta_c' \gamma$	117%	240%	117%	212%
$\chi_{c0} \rightarrow J/\Psi \gamma$	185%	357%	176%	307%
$\chi_{c1} \rightarrow J/\Psi \gamma$	15%	32%	10%	21%
$\chi_{c2} \rightarrow J/\Psi \gamma$	58%	119%	54%	97%
$\Psi(2S) \rightarrow \chi_{c0} \gamma$	65%	100%	68%	101%
$\Psi(2S) \rightarrow \chi_{c1} \gamma$	-17%	-24%	-15%	0%
$\Psi(2S) \rightarrow \chi_{c2} \gamma$	21%	33%	18%	27%

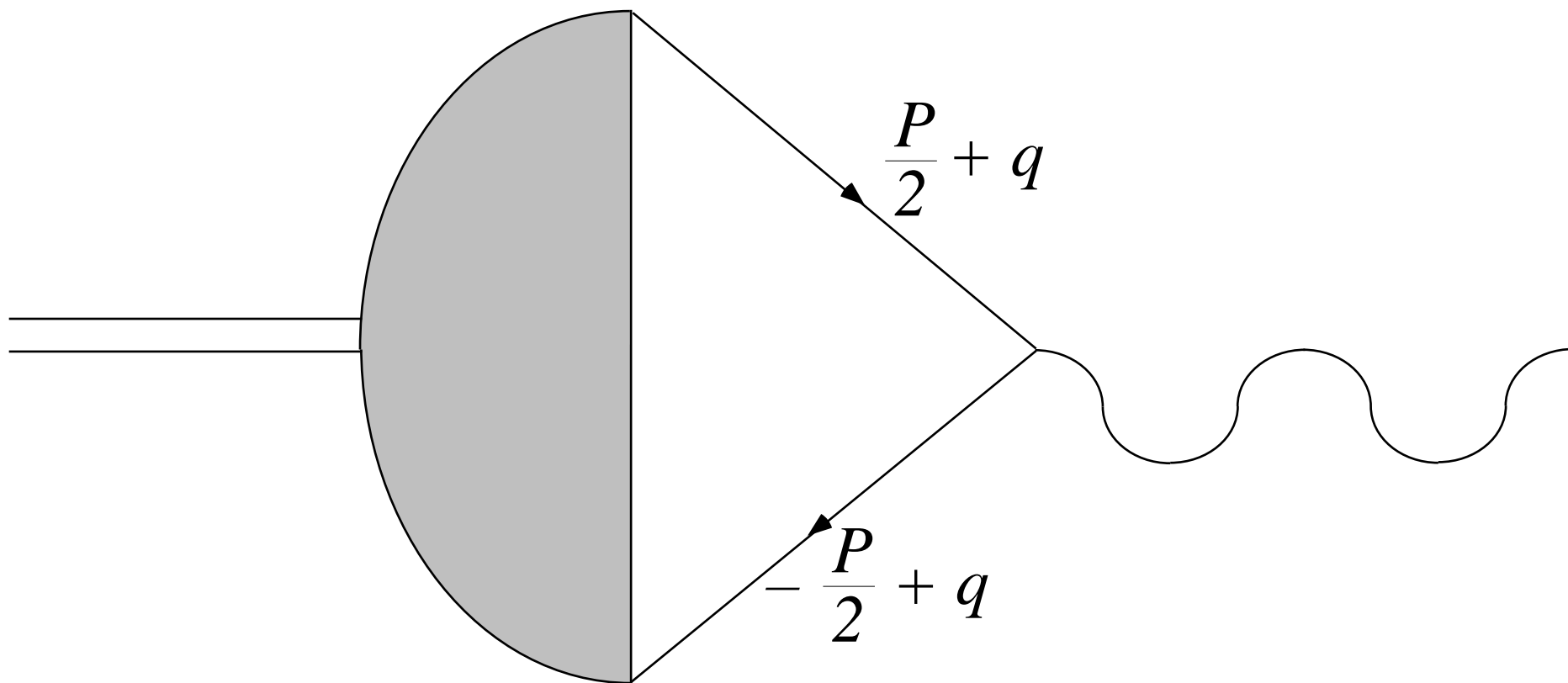


Figure 1

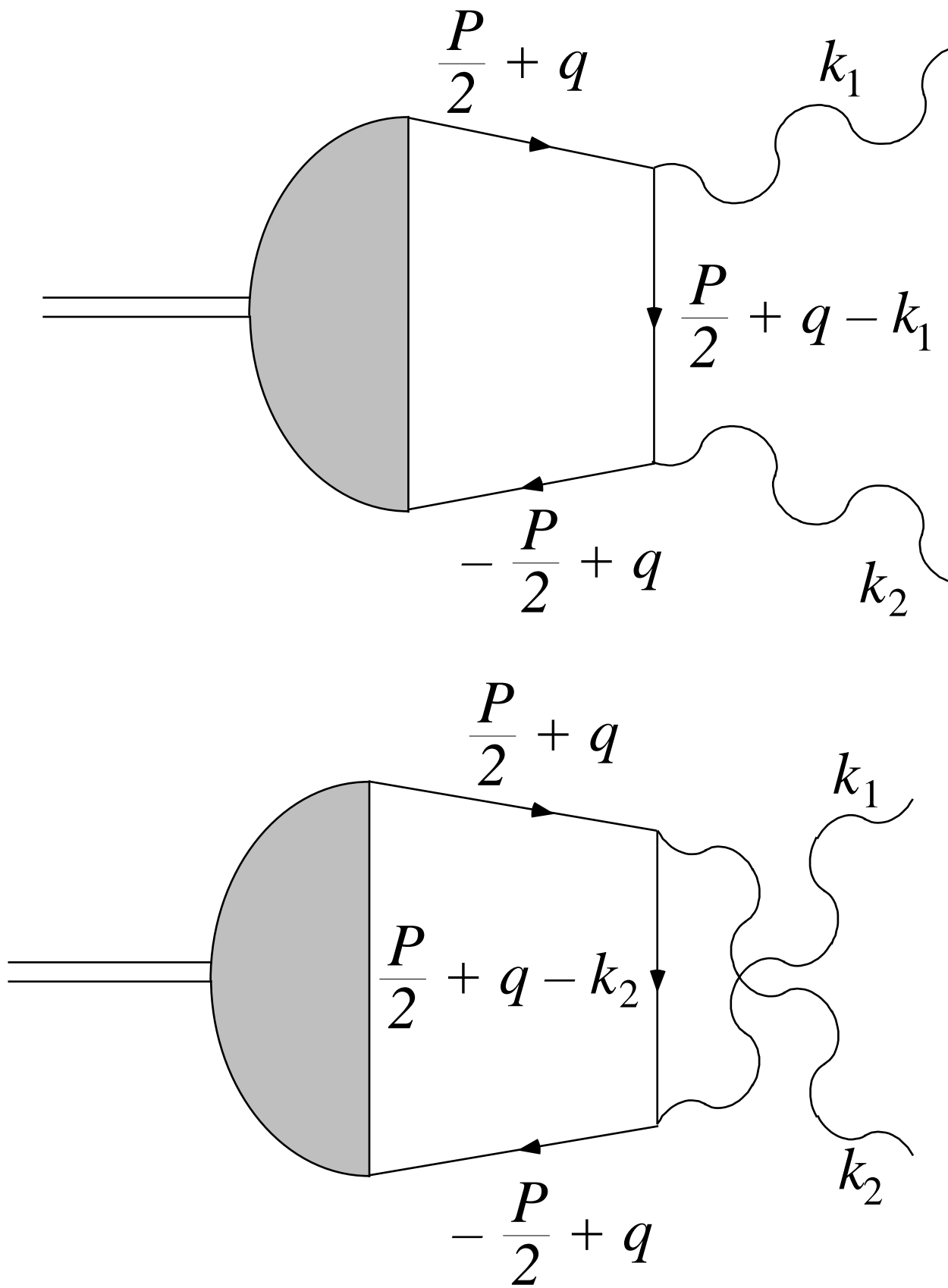


Figure 2

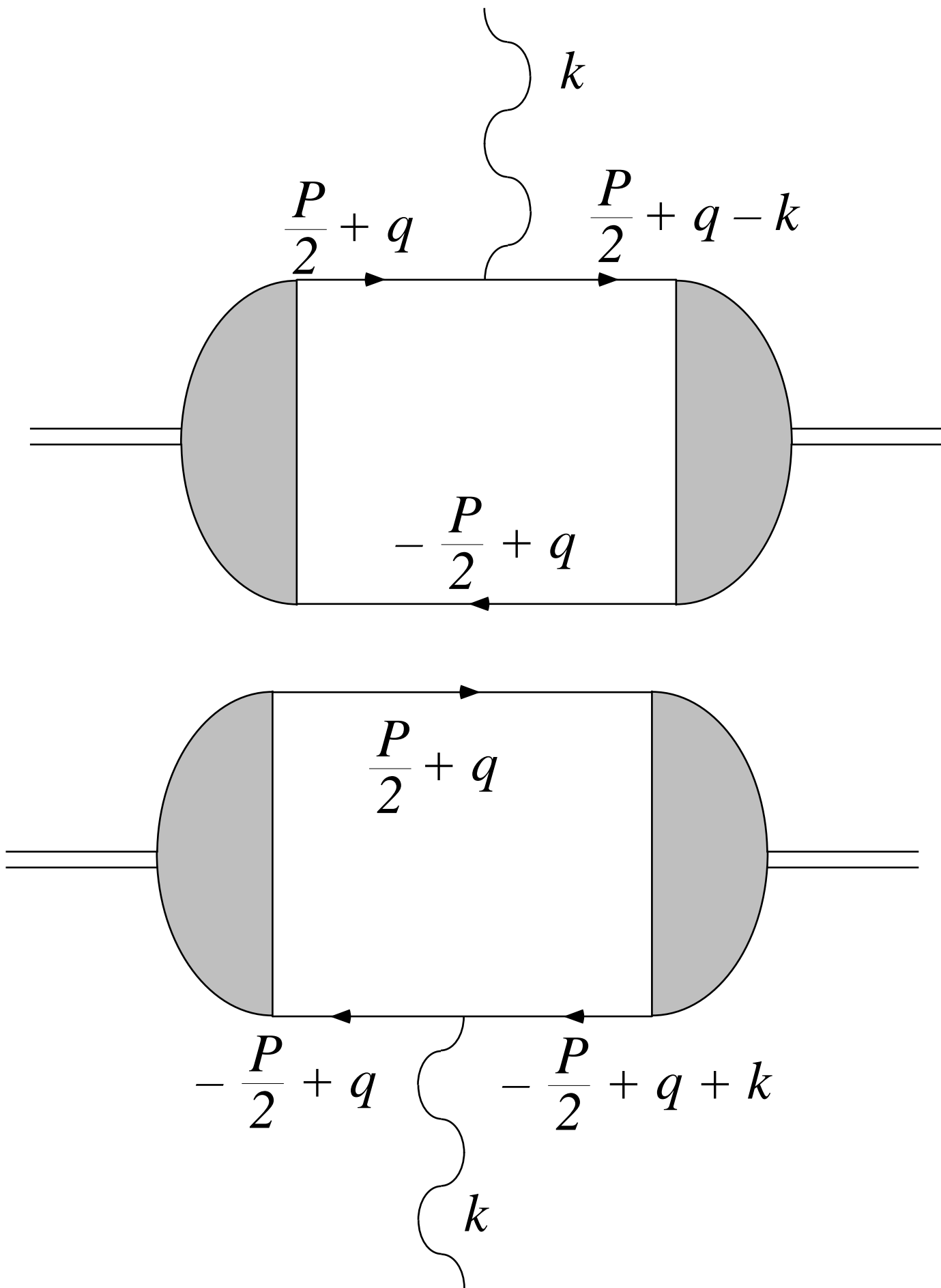


Figure 3

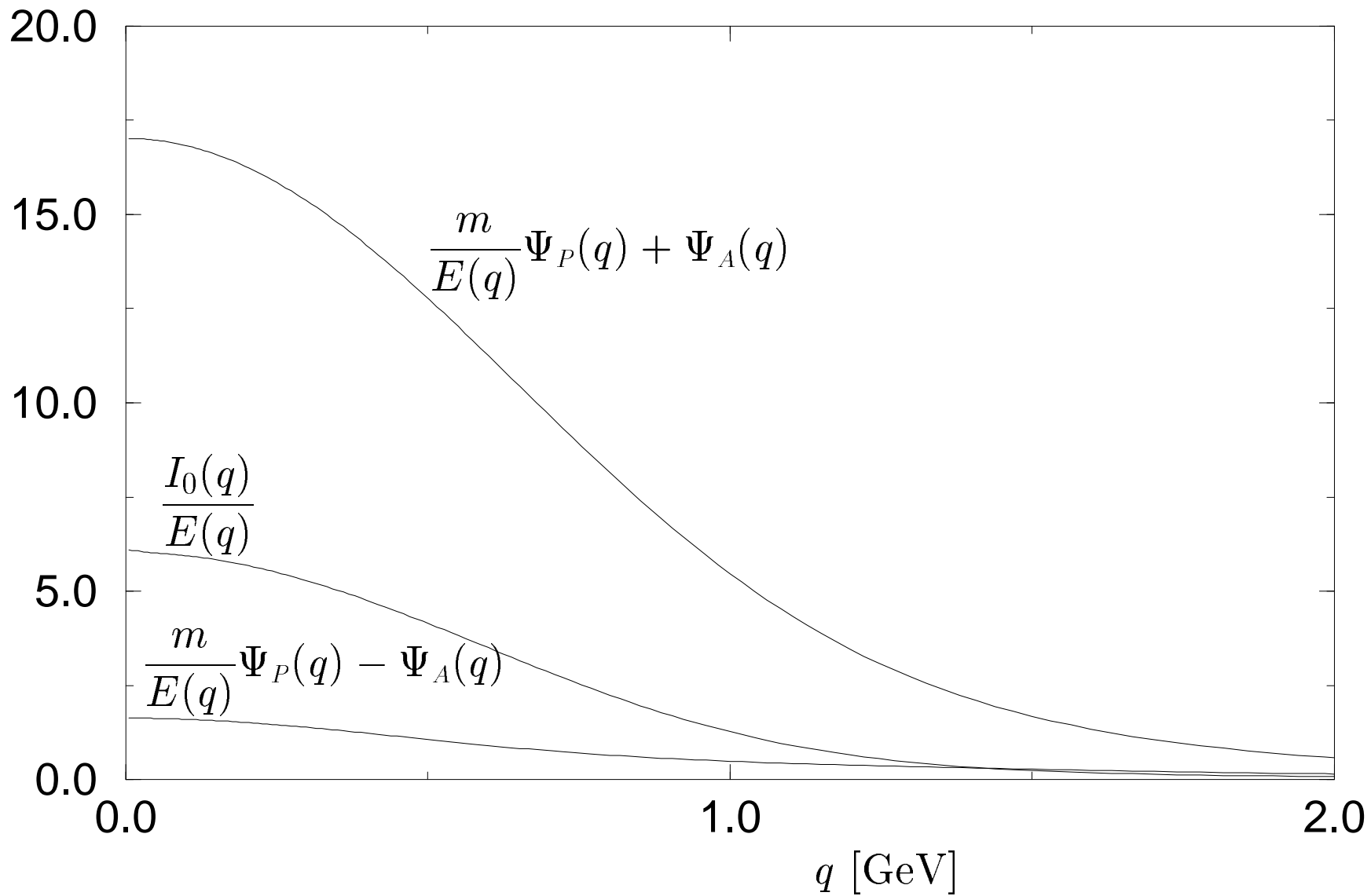


Figure 4